

7:30–8:00 AM Coffee and Pastries—Grand Assembly

Cases of the Day

Moderator: Melissa L. Rosado de Christenson, MD

7:30–7:45 AM Case of the Day
Kyung Soo Lee, MD

7:45–8:00 AM Case of the Day
Jane P. Ko, MD

8:00–11:00 AM **Workshops**

Track 1—Grand C

Moderator: Melissa L. Rosado de Christenson, MD

8:00–8:30 AM Mesothelioma (MPM): Update in Staging and Imaging
Jeremy J. Erasmus, MD

8:30–9:00 AM Peripheral Lung Disease: Living on the Edge
Jannette Collins, MD, MEd

9:00–9:30 AM The Radiologic and Pathologic Spectrum of Bronchopulmonary Carcinoids
Kay H. Vydareny, MD

9:30–10:00 AM Thoracic Cavitory Disease in the New Millennium
Humberto O. Martinez, MD

10:00–10:30 AM Neonatal Intensive Care Chest Radiology
George W. Gross, MD

10:30–11:00 AM Multichannel CT Pulmonary Angiography: Current and Future Directions
James F. Gruden, MD

11:00–11:30 AM Interventional Chest Radiology
Cristopher A. Meyer, MD

Track 2—Grand D

Moderator: Gerald F. Abbott, MD

8:00–8:30 AM Tricks of the Trade: Reading CXRs and CTs on a Workstation
David K. Shelton, Jr, MD

8:30–9:00 AM Congenital Pulmonary Vascular Anomalies: The Ins and Outs
Laura E. Heyneman, MD

9:00–9:30 AM Lobar Atelectasis: Radiographic CT Correlation
Kyung Soo Lee, MD

9:30–10:00 AM Recognition and Evaluation of Abnormal Cardiac Findings on Chest CT
Curtis E. Green, MD

10:00–10:30 AM Anterior Mediastinal Masses
Pierre D. Maldjian, MD

10:30–11:00 AM Pulmonary Aspergillosis: An Interconnected Spectrum
Irwin M. Freundlich, MD

Sunday

Mesothelioma (MPM): Update in Staging and Imaging

Jeremy J. Erasmus, MD

Introduction

Mesothelioma is an uncommon malignancy that arises from mesothelial cells of the pleura, pericardium and omentum. It is the most common primary neoplasm of the pleura with 7-13 new cases per million persons in the USA annually. The etiology is associated with asbestos inhalation and occupational exposure can be documented in 40-80% of patients. The tumor typically exhibits a propensity for local invasion and as a result patients often present with chest pain. Although the radiologic manifestations are variable, MPM characteristically manifests as an extra-parenchymal mass that is typically accompanied by a pleural effusion. Treatment depends on the extent of disease: most patients have extensive non-resectable tumor at presentation and are treated with chemotherapy and/or radiotherapy; pleurectomy or extrapleural pneumonectomy is performed in some patients when the tumor is confined to the pleural space. Prognosis is poor and demise of most patients usually occurs within one year of presentation.

This workshop will review the diagnosis, radiologic manifestations and staging of MPM.

Radiologic Evaluation

The most common radiographic manifestation of MPM, occurring in 30-80% of patients, is a unilateral pleural effusion that is small to large in size. Bilateral pleural effusions occur in 10% of patients. Mediastinal shift to the contralateral side is uncommon with large effusions because the diffuse extent of the tumor typically results in fixation of the mediastinum. More commonly, signs of volume loss of the ipsilateral hemithorax are present. The effusion often obscures the underlying pleura mass; the mass is usually smooth or lobular and typically encases the hemithorax. Discrete pleural masses occur occasionally and are typically multiple, rather than solitary. Lung and nodal metastases are late findings and are rarely detected radiographically.

CT manifestations of MPM include pleural effusion and pleural thickening which typically has a lower zone predominance and is more commonly nodular than smooth. CT findings that can be useful in distinguishing malignant from benign disease include circumferential pleural thickening and pleural thickening greater than 1 cm. CT can be useful in

detecting chest wall (16-18%) and mediastinal invasion (13%). CT manifestations of chest wall invasion include obscuration of fat planes, invasion of intercostal muscles, separation of ribs by tumor and bone destruction. Irregularity of the interface between the chest wall and the tumor is not, however, a reliable indicator of local invasion. CT assessment of invasion of the diaphragm and transdiaphragmatic extension of tumor is limited by the constraints of axial scanning. The most reliable CT sign for absence of local invasion is a clear fat plane between the inferior diaphragmatic surface and the adjacent abdominal organs and a smooth diaphragmatic contour. Conversely, a soft tissue mass encasing the hemidiaphragm is consistent with nonresectable disease. Invasion of vital structures such as great vessels, esophagus, heart and trachea, can manifest as obliteration of fat planes, direct invasion of mediastinal structures or the presence of tumor surrounding more than 50% of the circumference of the structure.

Although distant metastases are uncommon, intrathoracic metastases are common. Metastases are frequently present in peribronchial lymphatic vessels and peribronchial and mediastinal lymph nodes. CT has been reported to detect these metastases in 34-50% of patients. CT may underestimate nodal metastases as the nodes are often inseparable from adjacent mediastinal pleural thickening. Lung metastases typically manifest as nodules, masses or thickening of interlobular septa.

MR imaging can be useful in determining the presence and extent of disease. The sensitivity and specificity of MR imaging in predicting the malignant nature of diffuse pleural disease is 100% and 87% respectively. Because MPM typically has the same or slightly increased signal intensity to that of the adjacent chest wall muscle on T1-weighted images and moderately increased signal intensity on T2-weighted images, the use of gadolinium contrast enhancement can be useful in detecting disease. Furthermore, because MR imaging has the ability to image MPM in the coronal and sagittal planes, some studies have reported better delineation of diaphragmatic and apical chest wall regions than CT. MR imaging and CT were recently compared in a study of 65 patients with MPM and were found to be of nearly equivalent diagnostic accuracy in staging.

Evaluation of local invasion of adjacent structures had an accuracy of 50-65% for both CT and MR imaging. Accuracy in evaluation of N1 and N2 disease by both modalities was approximately 50%. Significant differences between CT and MR imaging were seen in only two categories: invasion of the diaphragm (CT accuracy 55%, MR 82%) and invasion of endothoracic fascia or a single chest wall focus of involvement (CT accuracy 46%, MR 69%). Consequently, imaging evaluation of patients with MPM is usually performed using CT. In those patients considered as surgical candidates, MR imaging is occasionally performed to evaluate pleural thickening involving the diaphragmatic surfaces. The additional information obtained may limit surgical exploration in patients with unresectable tumors, or guide the surgeon to investigate questionable areas of invasion before extrapleural pneumonectomy is undertaken.

Experience with radionuclide imaging using positron emission tomography and ^{18}F fluorodeoxyglucose (FDG-PET) in the evaluation of MPM is limited. Recently a small prospective study comparing FDG-PET imaging to CT was performed in patients suspected of having MPM. FDG uptake was significantly higher in MPM when compared to benign pleural disease (sensitivity 91%, specificity 100%) and showed improved detection of mediastinal nodal metastases. It is, however, doubtful whether FDG-PET imaging will replace morphological imaging in the assessment of MPM.

Invasive Procedures Utilized in Diagnosis

Pleural effusion analysis has limited utility in the diagnosis of MPM. Transthoracic needle biopsy of the pleura is also not optimal in establishing the diagnosis because of the difficulty in differentiating MPM from pleural sarcoma or metastatic adenocarcinoma. Obtaining larger tissue samples with imaging-guided biopsy improves the accuracy of diagnosis (accuracy 77-83%). Video-assisted thoracoscopic surgery (VATS) has become the preferred method for obtaining diagnostic specimens and in determining resectability. Although VATS has a diagnostic rate of 98%, the procedure has two disadvantages: (1) it requires that the visceral and parietal pleura not be adherent and; (2) chest wall seeding with tumor occurs in up to half of the patients (compared to only up to 22% by imaging guided biopsy).

Staging of Malignant Pleural Mesothelioma (MPM)

Previously proposed staging systems of MPM have tended to emphasize the importance of exten-

sive disease. Because of the increasing use of surgical resection to treat limited disease and the importance of nodal metastases in determining prognosis, the New International TNM Staging System for MPM has recently been proposed (Table 1, 2). This new staging system places greater emphasis on the importance of detecting early disease and by standardizing the description of the anatomic extent of disease, provides a framework for analyzing the results of prospective clinical trials. The New International TNM Staging System for MPM attempts to: (1) preoperatively identify patients with early disease (T1a, T1b) and a better prognosis and; (2) distinguish patients who may potentially benefit from surgery but not necessarily be cured (T2, T3), from those patients in whom surgery may not be beneficial because of extensive disease (local tumor spread - T4, locoregional disease - T4N3 or distant metastases - M1).

The new TNM staging system has limitations in achieving accurate evaluation of local and regional spread of MPM. CT or MR imaging cannot reliably determine many staging categories such as T1a, T1b and T2. Although MR imaging can occasionally improve staging evaluation of solitary foci of chest wall invasion, endothoracic fascia involvement and in revealing diaphragmatic muscle invasion, in most cases this does not alter surgical resection. Another limitation is that nodal status is usually unknown prior to surgery because: (1) CT and MR imaging have relatively low accuracy in detecting nodal metastases and (2) routine preoperative mediastinoscopy is not performed.

Postoperative Imaging

Fluid accumulation in the ipsilateral hemithorax following an extrapleural pneumonectomy is rapid with total opacification of the hemithorax typically occurring over several days. When fluid accumulates more rapidly than air can be reabsorbed, the mediastinum may shift to the contralateral side forcing air through the thoracotomy incision and simulating a bronchial stump leak/fistula. CT evaluation can be useful in differentiating recurrent disease from a surgical complication such as rupture of the reconstructed hemidiaphragm. Reconstruction of the resected diaphragm is often performed with a variety of materials such as Gore-Tex or latissimus dorsi muscle. In the early post-operative period the Gore-Tex prosthetic diaphragm appears as a radiolucent, crescent-shaped band and can be confused with a pneumoperitoneum. The prosthesis subsequently gradually becomes increasingly radio-opaque.

Table 1: New TNM International Staging System for Diffused MPM

T – Primary Tumor

- T1a Tumor limited to ipsilateral parietal pleura, including mediastinal and diaphragmatic pleura
No involvement of visceral pleura
- T1b Tumor involving ipsilateral parietal pleura, including mediastinal and diaphragmatic pleura
Scattered foci of tumor also involving visceral pleura
- T2 Tumor involving each ipsilateral pleural surfaces¹ with at least one of the following features:
 - involvement of diaphragmatic muscle
 - confluent visceral pleural tumor (including fissures) or extension of tumor from visceral pleura into underlying pulmonary parenchyma
- T3 Locally advanced but potentially resectable tumor
Tumor involving all of ipsilateral pleural surfaces¹ with at least one of the following:
 - involvement of endothoracic fascia
 - extension into mediastinal fat
 - solitary, completely resectable focus of tumor extending into soft tissues of chest wall
 - nontransmural involvement of pericardium
- T4 Locally advanced technically unresectable tumor
Tumor involving all of ipsilateral pleural surfaces¹ with at least one of the following:
 - diffuse extension or multifocal masses of tumor in chest wall, with or without associated rib destruction
 - direct transdiaphragmatic extension of tumor to peritoneum
 - direct extension of tumor to contralateral pleura
 - direct extension of tumor to one or more mediastinal organs
 - direct extension of tumor into spine
 - tumor extending through to internal surface of pericardium with or without pericardial effusion, or tumor involving myocardium

N – Lymph Nodes

- NX Regional lymph nodes not assessable
- N0 No regional lymph node metastases
- N1 Metastases in ipsilateral bronchopulmonary or hilar lymph nodes
- N2 Metastases in subcarinal or ipsilateral mediastinal lymph nodes, including ipsilateral internal mammary nodes
- N3 Metastases in contralateral mediastinal, contralateral internal mammary, and ipsilateral or contralateral supraclavicular lymph nodes

M - Metastases

- MX Distant metastases not assessable
- M0 No distant metastases
- M1 Distant metastases present

Table 2:

Stage	Description
Ia	T1aN0M0
Ib	T1bN0M0
II	T2N0M0
III	Any T3M0
	Any N1M0
	Any N2M0
IV	Any T4
	Any N3
	Any M1

Conclusion

The accurate assessment of the extent of malignant pleural mesothelioma is important in patient management. The New International TNM Staging System for MPM is being used to provide the framework for analyzing the results of prospective clinical trials. CT and MR imaging, despite limitations in accuracy, have an important role in this new staging system. CT is the standard imaging modality used to diagnosis and stage MPM, with MR imaging occasionally used to evaluate invasion of the hemidiaphragm, chest wall and mediastinum.

REFERENCES

1. Benard F, Sterman D, Smith RJ, et al. Metabolic imaging of malignant pleural mesothelioma with fluorodeoxyglucose positron emission tomography. *Chest* 1998;114:713-722.
2. Grondin SC, Sugarbaker DJ. Pleuropneumonectomy in the treatment of malignant pleural mesothelioma. *Chest* 1999 116:450S-454S.
3. Falaschi F, Battolla L, Mascalchi M, et al. Usefulness of MR signal intensity in distinguishing benign from malignant pleural disease. *AJR* 1996;166:963-968.
4. Helio A, Stenwig AE, Solheim OP. Malignant pleural mesothelioma: US-guided histologic core-needle biopsy. *Radiology* 1999;211:657-659.
5. Heelan RT, Rusch VW, Begg CB, et al. Staging of malignant pleural mesothelioma: comparison of CT and MR imaging. *AJR* 1999;172:1039-1047.
6. Metinas M, Ozdemir N, Isiksoy S, et al. CT-guided pleural needle biopsy in the diagnosis of malignant mesothelioma. *JCAT* 1995;19:370-374.
7. Miller BH, Rosado-de-Christenson ML, Mason AC, et al. Malignant pleural mesothelioma: radiologic-pathologic correlation. *RadioGraphics* 1996;16:613-644.
8. Ohishi N, Oka T, Fukuhara T, et al. Extensive pulmonary metastases in malignant pleural mesothelioma: a rare clinical and radiographic presentation. *Chest* 1996;110:296-8.
9. Patz EF Jr, Rusch VW, Heelan R. The proposed new international TNM staging system for malignant pleural mesothelioma: application to imaging. *AJR* 1996;166:323-327.
10. Rusch VW, Venkatraman ES. Important prognostic factors in patients with malignant pleural mesothelioma managed surgically. *Ann Thorac Surg* 1999;68:1799-804.

Peripheral Lung Disease: Living on the Edge

Jannette Collins, MD, MEd

Learning Objective

Recognize a pattern of peripheral lung disease on radiography or CT scanning of the chest and give an appropriate differential diagnosis, including a single most likely diagnosis when supported by associated radiologic findings or clinical information.

The diseases discussed in this presentation are not ordinarily grouped together. Alveolar sarcoidosis, idiopathic pulmonary fibrosis, pulmonary contusion, eosinophilic pneumonia, bronchiolitis obliterans organizing pneumonia (BOOP), and pulmonary infarct are discussed together because of their propensity for producing a predominantly peripheral distribution of disease on radiography and CT scanning of the chest. This distribution of disease can help in narrowing the differential diagnosis. A simple mnemonic of “AEIOU” can be used to remember disorders having a peripheral distribution of disease (Table). It needs to be said, however, that these disorders frequently do not manifest as peripheral opacities on chest radiography or CT scanning, and the lack of peripheral opacities will not exclude these disorders.

Table. Disorders manifesting as peripheral opacities on radiography or CT scanning of the chest

“AEIOU”
Alveolar sarcoidosis
Eosinophilic pneumonia
Infarcts
BOOP
UIP
ContUision

Alveolar Sarcoidosis

Sarcoidosis is a systemic disease of unknown etiology, characterized by widespread development of noncaseating granulomas. The typical radiologic appearance of pulmonary sarcoidosis is reticulonodular opacities in a lymphatic distribution, with or without hilar or mediastinal lymphadenopathy. This presentation will be limited to a discussion of those patients with sarcoidosis who have “alveolar” opacities on radiography or CT scanning of the chest.

Although the term “alveolar” sarcoidosis is used, the process is interstitial with compression and obliteration of alveoli, creating the appearance of alveolar filling on radiologic imaging. Histologically, these lesions are seen to represent confluent interstitial granulomas. Airspace (alveolar) opacities develop in 10% to 20% of patients with sarcoidosis. The typical radiologic appearance is that of bilateral, multifocal, poorly defined opacities, ranging in size from 1 to 10 cm, with a predilection for the peripheral mid lung zones, sparing the costophrenic angles [1]. The peripheral distribution is better seen, and on occasion only appreciated on CT scanning. Air bronchograms are common. Most patients with alveolar sarcoidosis have accompanying lymphadenopathy [2]. When only peripheral opacities are seen, the appearance can be indistinguishable from BOOP or eosinophilic pneumonia. Although all three disorders can present with blood eosinophilia, the degree of eosinophilia is most pronounced with eosinophilic pneumonia. The peripheral opacities of alveolar sarcoidosis can clear rapidly with or without steroid treatment [1].

Eosinophilic Pneumonia

The term “pulmonary eosinophilia”, synonymous with “pulmonary infiltration with eosinophilia” (PIE), describes a group of diseases in which blood and/or tissue eosinophilia affects major airways and lung parenchyma. Blood eosinophilia, however, is not necessary to make a diagnosis of eosinophilic lung disease. The number of diseases included under the umbrella term “pulmonary eosinophilia” are numerous. This presentation will focus on idiopathic pulmonary eosinophilia.

Cryptogenic (idiopathic) eosinophilic pneumonia (EP) can be acute or chronic, depending on whether the condition lasts more or less than one month. However, the 1-month criterion is arbitrary, and the distinction between acute and chronic EP is not always clear.

Acute EP, also referred to as Löffler’s syndrome, is characterized by blood eosinophilia, absence of or mild symptoms and signs (cough, fever, dyspnea), one or more nonsegmental mixed interstitial and alveolar pulmonary opacities that are transitory or migratory, and spontaneous clearing of opacities (within 1 month). The pulmonary opacities have a tendency to be predominantly peripheral in distribution. One

way of remembering this peripheral distribution is to think of “EP” (eosinophilic pneumonia) as being the opposite of “PE” (pulmonary edema). The classic distribution of pulmonary edema is a central “batwing” or “butterfly” pattern of alveolar lung disease, just the opposite of the peripheral alveolar opacities seen with eosinophilic pneumonia. Pleural effusions and lymphadenopathy are not features of acute EP.

Chronic EP is most prevalent in the third to seventh decades of life, with women outnumbering men 2 to 1 [3]. Symptoms of dyspnea, cough, wheeze, malaise, weight loss, fever, and night sweats can be mild or severe. Blood eosinophilia occurs in the majority of patients. Serum IgE is normal or only mildly elevated, which is helpful in distinguishing the condition from allergic bronchopulmonary aspergillosis and tropical and parasitic pulmonary eosinophilias, in which serum IgE levels are markedly elevated. The classic radiographic and chest CT scan finding is peripheral, nonsegmental, homogeneous alveolar opacities, often with air bronchograms [4]. In a minority of patients, the opacities will be central in distribution, or be both central and peripheral. Chronic EP is sensitive to steroid therapy, and rapid clearing of radiologic abnormalities is usually seen within a few days, with complete clearing by 1 month. Relapse is common, and the majority of patients need long-term low-dose steroids, distinguishing this disease from acute EP.

Pulmonary Infarction and Thromboembolism

Radiographic changes detected in a patient with pulmonary embolism are usually related to pulmonary infarction. Only 15% or less of thromboemboli cause pulmonary infarction [5]. It is unknown why some emboli cause infarction and others do not, but it is likely due to compromise of both the pulmonary and bronchial arterial circulation, which is most likely to occur with peripheral emboli and in patients with heart failure or circulatory shock. It is known that bronchial circulation alone can sustain the lung parenchyma without infarction occurring.

No chest radiographic sign is specific for pulmonary embolism or infarction and the sensitivity of chest radiography for these conditions is poor. Even with large pulmonary artery clot burden, the chest radiograph can be normal. The main role of the chest radiograph, therefore, is to exclude other diagnoses that might mimic pulmonary embolism clinically, such as pneumonia or pneumothorax.

Pulmonary infarction results in airspace opacities that are usually multifocal and predominantly in the lower lung zones. They usually appear within 12 to 24 hours after the embolic event. The opacities are

classically peripheral, have a triangular or rounded shape (thus the term “Hampton’s hump”), and are always in contact with the pleural surfaces [6]. The apex of the opacity is directed towards the lung hilum. Occasionally, lobar consolidation resembling pneumonia can occur. Air bronchograms are rarely present. It is important to note that the opacities can be a result of pulmonary hemorrhage without infarction, in which case clearing occurs within a week. Infarction takes several months to resolve, often with residual scarring. As infarcts resolve, they “melt away like an ice cube” (giving rise to the “melting ice cube sign”). The opacity clears from the periphery first, whereas in pneumonia, the opacity clears homogeneously, both centrally and peripherally at the same time. Cavitation can occur within infarcts, but is rare without co-existing infection, either secondary infection of an infarct or a result of septic emboli. Pleural effusions related to pulmonary embolism are usually small, unilateral, and associated with pulmonary infarction.

CT findings of acute pulmonary embolism include non-enhancing thrombus, manifested as a filling defect within an often-enlarged pulmonary artery, and peripheral pulmonary opacities consistent with pulmonary infarct in the subtending lung. Clot that is eccentric, along the wall of the pulmonary artery, indicates chronic thromboembolic disease from clot that been re-canalized. Additional CT findings include: 1) clot within the cardiac chambers or inferior vena cava, 2) right heart enlargement in cases of massive acute thromboemboli and acute right heart failure, 3) enlarged pulmonary arteries from chronic emboli and pulmonary artery hypertension, and 4) a mosaic pattern of lung attenuation on high-resolution CT indicating diminished perfusion in areas of lung supplied by pulmonary arteries involved with chronic thromboembolic disease.

Bronchiolitis Obliterans Organizing Pneumonia

Bronchiolitis obliterans organizing pneumonia (BOOP), also referred to as cryptogenic organizing pneumonia (COP), is a clinicopathologic entity of unknown cause characterized by clinical symptoms of cough and dyspnea, and chest radiographic findings of patchy, peripheral airspace opacities. Although often idiopathic in etiology, several precipitating conditions have been identified, including infections, connective tissue disorders, drug toxicity, inhalation of noxious fumes, and lung and bone marrow transplantation. Patients with idiopathic BOOP are generally 55 to 60 years of age, and half of patients have a history of an influenza-like prodrome followed by a short illness of about 3 months

characterized by cough, exertional dyspnea, malaise, fever, and weight loss [7].

Radiographs and CT scans of the chest show bilateral, patchy, nonsegmental, airspace opacities with a peripheral and basilar predominance [8]. The opacities may contain air bronchograms. On occasion, the opacities are not peripheral in distribution, but are central, and centered along bronchovascular bundles. Areas of ground glass attenuation are common, and can be the only finding on CT scanning.

Idiopathic Pulmonary Fibrosis

In 1965, Liebow classified the chronic interstitial pneumonias, including usual interstitial pneumonia (UIP) and desquamative interstitial pneumonia (DIP). Idiopathic pulmonary fibrosis (IPF, cryptogenic fibrosing alveolitis) occurs most commonly in patients between 40 and 60 years of age with progressive shortness of breath and dry cough. Pathologically, the majority of patients with IPF show typical histologic findings of usual interstitial pneumonia: a patchy distribution of active inflammation or alveolitis (or normal lung) and end-stage fibrosis. DIP is associated with a large number of macrophages in the alveolar spaces, and is more homogeneous than UIP in distribution on histologic specimens. DIP was termed "desquamative interstitial pneumonitis" because it was originally thought that the intra-alveolar cells were desquamated type II pneumocytes.

The chest radiographic findings are similar for both UIP and DIP [9], although the abnormalities are generally less severe with DIP. DIP has a better prognosis, and more patients with DIP respond to treatment with steroids than do patients with UIP [9].

With both UIP and DIP, the radiograph may be normal or show ground glass opacities or reticular interstitial opacities, primarily at the lung bases and subpleural areas. Both can progress to end-stage pulmonary fibrosis with honeycombing and traction bronchiectasis. The HRCT findings in IPF include irregular interlobular septal thickening, intralobular interstitial thickening, irregular interfaces, visible intralobular bronchioles, honeycombing, traction bronchiectasis, and ground glass opacities with a peripheral and subpleural predominant distribution. The predominant HRCT finding in DIP is ground glass opacification in a lower lung zone distribution.

Pulmonary Contusion

Abnormal lung opacification in patients sustaining trauma to the chest can result from atelectasis, aspiration, edema, pneumonia, and lung injury (contusion and laceration), and is commonly multifactorial in etiology. Pulmonary contusion ("lung bruise") results in leakage of blood and edema fluid into the interstitial and alveolar spaces. CT is more sensitive than radiography in demonstrating pulmonary contusion [10]. On both chest radiography and CT, pulmonary contusions present as areas of consolidation, ground glass opacification, or both, that tend to be peripheral, nonsegmental, and geographic in distribution. Contusions are evident at presentation or within six hours, and resolve, usually without permanent sequelae, within days to weeks.

REFERENCES

1. Battesti JP, Saumon G, Valeyre D, et al. Pulmonary sarcoidosis with an alveolar radiographic pattern. *Thorax* 1982; 37:448-452.
2. Kirks DR, McCormick VD, Greenspan RH. Pulmonary sarcoidosis: roentgenologic analysis of 150 patients. *AJR* 1973; 117:777-786.
3. Jederlinic PJ, Sicilian L, Gaensler EA. Chronic eosinophilic pneumonia: a report of 19 cases and a review of the literature. *Medicine* 1988; 67:154-162.
4. Mayo JR, Müller NL, Road J, et al. Chronic eosinophilic pneumonia: CT findings in six cases. *AJR* 1989; 153:727-730.
5. Moser KM. Pulmonary embolism: state of the art. *Am Rev Respir Dis* 1977; 115:829-852.
6. Hampton AO, Castleman B. Correlations of post mortem chest teleroentgenograms with autopsy findings with special reference to pulmonary embolism and infarction. *AJR* 1940; 43:305-326.
7. King TE, Mortenson RL. Cryptogenic organizing pneumonitis: the North American experience. *Chest* 1992; 102(suppl):8S-13S.
8. Izumi T, Kitaichi M, Nishimura K, et al. Bronchiolitis obliterans organizing pneumonia: clinical features and differential diagnosis. *Chest* 1992; 102:715-719.
9. Carrington CB, Gaensler EA, Coute RE, Fitzgerald MS, Gupta RG. Natural history and treated course of usual and desquamative interstitial pneumonia. *N Engl J Med* 1978; 298:801-809.
10. Schild HH, Strunk H, Weber W, et al. Pulmonary contusion: CT vs plain radiograms. *J Comput Assist Tomogr* 1989; 13:417-420.

The Radiologic and Pathologic Spectrum of Bronchopulmonary Carcinoids

Kay H. Vydareny, MD

Objectives

Following this workshop, the audience will:

1. Be able to describe the radiologic appearance of bronchopulmonary carcinoids.
2. Know the histologic differences between typical and atypical pulmonary carcinoids.
3. Know the prognostic difference between typical and atypical carcinoids.

Bronchopulmonary carcinoids are uncommon pulmonary malignancies representing 1-2% of all lung tumors. They are neuro-endocrine tumors, felt to arise from a pluripotential stem cell. Although they present with a common clinical and radiologic pattern, they have a spectrum of pathologic patterns which show varying degrees of malignancy ranging from the low grade typical carcinoid, to the intermediate grade atypical carcinoid, to the higher grade large cell neuroendocrine tumor and small cell carcinoma.

Clinical Presentation

Bronchopulmonary carcinoids present in a wide age range, predominantly in the third to seventh decades. The average age at presentation is 45.5 years, younger than the usual age for bronchogenic carcinoma. Patients with atypical carcinoids tend to present at an older age than do those with typical carcinoids. The male:female ratio is nearly 1:1. Whites are affected more than blacks and there is no known association with cigarette smoking.

Up to 50% of the patients, typically those with peripheral tumors, are asymptomatic. The others, especially those with central tumors, present with a variety of symptoms typically caused by endobronchial obstruction. Thus, recurrent pneumonia or atelectasis and wheezing in one lung are common. Although the tumors usually have an intact overlying mucosa, they are very vascular and hemoptysis is common. Sputum cytology is rarely useful in the diagnosis.

Paraneoplastic syndromes are uncommon. The carcinoid syndrome, which includes flushing, diarrhea, abdominal cramping, wheezing and cardiac disease, almost always occurs in patients with liver metastasis and is uncommon with thoracic carcinoids. When it does occur, it is more frequent in patients with typical carcinoids. Up to 2% of patients can

present with Cushing's syndrome due to production of ectopic ACTH or ACTH releasing hormone by the tumor. Indeed, bronchial carcinoids are the most common source of ectopic ACTH production.

Radiologic Presentation

There is no difference in the radiologic presentation of typical and atypical carcinoid tumors. Carcinoids occur both centrally (85% of tumors arise in the main or, most commonly, the lobar bronchi) and in the periphery of the lung. Most carcinoids are central and present as a hilar or perihilar mass. On chest x-ray, the mass is smooth or lobulated and may have a notched contour. A spiculated mass, typical of bronchogenic carcinoma, is rarely seen. Because of the endobronchial component of the mass, there is often associated atelectasis, post-obstructive consolidation, or mucoid impaction. Peripheral tumors are also sharply demarcated, usually ovoid nodules surrounded by aerated lung.

On CT, calcification or ossification can be seen in nearly 40% of the central lesions. Peripheral tumors, which are more likely to represent atypical carcinoid, are less likely to be calcified. Most tumors are round. When they are ovoid, they tend to be oriented with their long axis parallel to the nearest bronchus or pulmonary artery. Because of their vascularity, carcinoids usually show marked enhancement following injection of contrast material. Many carcinoids are both endobronchial and extrabronchial; in fact, the endobronchial component may be very small relative to the extrabronchial component. CT allows visualization of the entire lesion and of its effects (e.g. mucus plugging, atelectasis or post-obstructive consolidation).

Carcinoids typically have a large number of somatostatin binding sites. ¹¹¹Indium octreotide, a somatostatin analog, can be used for scintigraphic localization both of the primary tumor and lymph node metastases, and can be useful in detecting functionally active small tumors not visible on CT.

Metastatic disease occurs more frequently in atypical carcinoids than in typical carcinoids (46.4% vs. 23.1%) (4). The most frequent sites of metastases are to lymph nodes and liver. Metastases may also involve bone, lung and adrenals.

Pathology

Typical carcinoids are composed of uniform cells in a rich fibrovascular stroma. There are fewer than two mitoses per 10 high power fields and there may be dystrophic calcification or ossification. They are highly vascular. Electron microscopy reveals neurosecretory granules which are more common and larger than in atypical tumors.

Atypical carcinoids comprise approximately 10% of all carcinoids and demonstrate more active mitoses (2-19 per 10 high power fields). There may be architectural distortion and tumor necrosis. Although both typical and atypical carcinoids metastasize to regional lymph nodes and may invade blood or lymph vessels, atypical tumors do so more frequently and more aggressively.

Typical and atypical carcinoids cannot be distinguished by their gross anatomical appearance.

Treatment and Prognosis

The treatment for the patient with any type of carcinoid is surgical excision. The prognosis of patients

with typical carcinoid is excellent with studies showing 84-95% ten-year survival for typical carcinoids and 44-60% ten-year survival for atypical tumors. Tumor size larger than 3 cm. and nodal metastases adversely affect survival.

REFERENCES

1. Dusmet ME, McKneally MF. Pulmonary and thymic carcinoid tumors. *World J of Surg* 1996; 20:189-195.
2. Gould PM, Bonner JA, Sawyer TE, Deshcamps C, Lange CM, Li H. Bronchial carcinoid tumors: importance of prognostic factors that influence patterns of recurrence and overall survival. *Radiology* 1998; 208:1, 181-185.
3. Rosado de Christenson M., Abbot GF, Kirejczyk WM, Galvin JR, Travis WD. Thoracic carcinoids; radiologic-pathologic correlation. *Radiographics* 1999; 19:3, 707-736.
4. Soga J, Yakuwa Y. Bronchopulmonary carcinoids: an analysis of 1875 reported cases with special reference to a comparison between typical carcinoids and atypical varieties. *Ann Thorac Cardiovasc Surg* 1999; 5:4, 211-219.
5. Zwiebel BR, Austin JHM, Grimes MM. Bronchial carcinoid tumors: assessment with CT of location and intratumoral calcification in 31 patients. *Radiology* 1991; 179:2, 483-486.

Thoracic Cavitory Disease in the New Millennium

Humberto O. Martinez, MD

The AIDS epidemic has already introduced us to opportunistic infectious organisms, such as *Pneumocystis carinii*, which has become a prevalent cause for pulmonary cavities. In the new millennium, as immunocompromised patients live longer with new treatment protocols, we will be challenged with the diagnoses of new causes of cavitory thoracic disease. Tuberculosis is once again one of the most common cavitory infections in the normal immune host. Therefore, it is not only important to be familiar with the differential diagnoses of thoracic lucent defects, but also the role of plain film imaging of the chest and cross-sectional imaging particularly as it pertains to the distinction of parenchymal lesions from those caused by pleural or extra-pleural disease.

A true cavity is a gas filled space resulting from necrosis of lung parenchyma within a zone of consolidation, a nodule, or a mass, with liquefaction and evacuation of contents via the tracheo-bronchial tree. A true cavity can be differentiated from a pulmonary air cyst in that the later usually presents with well defined walls no greater than 2 mm thick and larger than 1 cm in diameter.¹ Radiographically, pulmonary cavities can present as single or multiple lesions varying in size and wall thickness and may or may not be associated with surrounding parenchymal infiltration. The most useful criterion in differentiating neoplastic from non-neoplastic cavitory lung disease is cavity wall thickness (measured at the thickest point). Other criteria useful in narrowing the differential diagnosis of cavitory lung disease include the presence of single or multiple lesions, as well as the presence of a surrounding infiltrate.

Many entities can give rise to cavitory lesions in the lung. These may be solitary or multiple and include infectious, inflammatory, and neoplastic etiologies. Often the most important question the Radiologist can answer is whether the lesion is neoplastic or non-neoplastic. Several studies have previously reported radiographic criteria to help differentiate benign from malignant lesions. Cavities with wall thickness greater than 15 mm were malignant in 95% of the cases, whereas those 4 mm. or less were benign in greater than 92% of the cases. All cavities with wall thickness of 1 mm. or less were benign. Those having wall thickness between 5 to 15 mm. had a 50% chance of being benign or malignant.²

Other entities can present as lucent defects in the thorax which mimic cavitory lung disease. Etiologies include pleural disease such as empyema and loculated pneumothorax. Post surgical entities such as post-pneumonectomy space, plombage thoracoplasty, gastric pull-up, post traumatic causes such as traumatic rupture of diaphragm with herniating bowel in to the chest; and congenital causes such as diaphragmatic hernias.

The other radiographic criteria useful in narrowing the differential diagnosis of cavitory lung disease analyze the presence of single or multiple cavitory lesions. The presence of a single thick wall cavitory mass usually implies malignancy, whereas the presence of multiple thin wall cavities usually implies benign disease such as an inflammatory or infectious process.

The following table lists several causes of lucent defects in the thorax:

- Congenital and Neonatal Diseases
 - Bronchopulmonary dysplasia
 - Wilson-Mikity syndrome
 - Cystic adenomatoid malformation
 - Pulmonary sequestration
- Airways Diseases
 - Bullous emphysema
 - Cystic bronchiectasis
- Infectious Diseases
 - Tuberculosis and atypical mycobacterial infections
 - Fungal infections: coccidioidomycosis, cryptococcosis, aspergillosis, blastomycosis, Staphylococcal pneumonia causing pneumatoceles
 - Gram-negative pneumonias causing pneumatoceles
 - Parasitic diseases: echinococcosis
 - Opportunistic Infections: *Pneumocystis carinii*
 - Others: nocardiosis
- Embolic Diseases
 - Pulmonary thromboembolism
 - Septic embolism
- Neoplastic Diseases
 - Hematogenous metastases
 - Pulmonary spread of laryngeal papillomatosis
 - Hodgkin's disease and non-Hodgkin's lymphoma
 - Primary lung tumor (especially squamous cell)

Autoimmune Diseases

- Rheumatoid necrobiotic nodules
- Wegener's granulomatosis
- Polyarteritis nodosa (very rare)

Diseases of unknown origin

- Sarcoidosis
- Histiocytosis X

Trauma

- Hydrocarbon ingestion with pneumatocele formation
- Traumatic lung cysts (pulmonary laceration)

Conditions Mimicking Cavities

- Herniation of bowel into the thorax
- Air-containing empyema
- Lucite plombage

REFERENCES

1. Armstrong Pt Wilson AG, Dee P. Infections of the lungs and pleura. In: Imaging of diseases of the chest. Chicago, Year Book Medical Publishers, Inc.,1991; 172.
2. Boiselle PM,Crans CA,Kaplan MA. The changing face of Pneumocystis carinii pneumonia in AIDS patients. AJR 1999; 1301-1309
3. Fraser RGI Pare JAP, Pare PD, Fraser RS, Genereux GP. Diagnosis of diseases of the chest. 3rd ed., Philadelphia, Saunders Co, 1991(4).
3. Freundlich IM. Abscesses, pulmonary masses, cysts & cavities: a radiologic approach. Chicago, Year Book Medical Publishers, Inc.,1981; 72
4. Freundlich IM, Bragg DG. An approach to the diagnosis of thoracic abnormalities: cysts and cavities of the lung. In: A radiological approach to diseases of the chest. Baltimore, Williams & Wilkins, 1992; 96.
5. Godwin DJ, Webb RW, Savoca CJ, Gamsu G, Goodman PC. Review: Multiple, thin walled cystic lesions of the lung. AJR 1980; 135:593-604.
6. Greene R. Opportunistic pneumonosis. Semin Roentgenol 1980; 15(1).
7. Jules-Glysee KMI Stuver DE, Muhammad ZB,etal. Aerosolized pentamidine: effect on diagnosis and presentation of pneumocystis carinii pneumonia. Ann Intern Med 1990; 112:750-757.
8. Saldana MJ, Mones JM. Cavitation and other atypical manifestations of pneumocystis carinii pneumonia. Semin Diagn Pathol 1989; 6(3):273-286.
9. Wolinsky E. Nontuberculous mycobacteria and associated diseases. Am Rev Respir Dis 1979; 119:107.
10. Woodring JH, Fried AM, Chuang VP. Solitary cavities of the lung: diagnostic implications of cavity wall thickness. AJR 1980; 135:1269-1271.

Workshop: Neonatal Intensive Care Chest Radiology

George W. Gross, MD

This workshop will include discussion of the following topics with examples of the more common and/or important problems and issues:

1. Technical aspects of neonatal chest imaging, including equipment and projections
2. Radiation exposure and protection
3. Catheters, tubes, and monitors employed in the NICU
4. Normal appearances and normal variants
5. The most common and/or important “medical” and “surgical” pulmonary disorders in newborns
6. Findings suggestive of congenital cardiac disease
7. Newer support techniques used in the NICU
8. Use of ultrasonography of the thorax in the NICU

BIBLIOGRAPHY

1. Gross, GW. Radiology in the Intensive Care Nursery, pp 345-400. In: Intensive Care of the Fetus and Neonate. Ed: A. R. Spitzer, Mosby. St. Louis. 1996
2. Swischuk LE. Imaging of the Newborn, Infant, and Young Child. Williams and Wilkins. Baltimore. 1989
3. Gross, GW. Chest imaging in the neonatal and pediatric intensive care units. *Resp Care* 1999; 44(9):1095-1126.

Multi-channel CT Pulmonary Angiography: Current and Future Directions

James F. Gruden, MD

Associate Professor of Radiology and Internal Medicine

Emory University School of Medicine

Adjunct Professor, Biomedical Engineering

Georgia Institute of Technology

Division Director, Cardiothoracic Imaging and Diagnosis

Emory University Hospital and Clinic, Grady Memorial Hospital

404-712-7964

jgruden@emory.edu

Objectives

1. To understand the fundamental differences and similarities between single and four channel helical CT angiography and the advantages each has over conventional angiography and scintigraphy and to know the scientific basis for these advantages.
2. To identify current areas of research in image display and processing of large volumetric data sets that may enhance our ability to diagnose thromboembolic disease.

Background

During the period 1984-1991, an average of 50,000 cases of pulmonary embolism were diagnosed each year in the hospitalized Medicare population alone with a mortality rate of at least 10%.¹ Definitive diagnosis is of paramount importance because of both the seriousness of the condition itself and because complications of anticoagulant therapy are frequent and can be severe.

Definitive diagnosis or exclusion of PE remains problematic, and there are few areas of medicine with such a significant level of uncertainty and confusion with regard to accurate diagnosis and therapy. One autopsy study found that only 10% of patients 70 years of age and older with PE had a correct diagnosis before death.² Missed diagnosis is not the only problem; *of all patients with an ICD-9 discharge diagnosis of PE in one series, 28% had no objective evidence of either PE or deep venous thrombosis (DVT).*³

These diagnostic inaccuracies exist for two major reasons. First, the clinical signs and symptoms asso-

ciated with PE are nonspecific, as are laboratory investigations, electrocardiograms, and chest radiographs. Clinical studies show a high prevalence of symptoms in patients with PE because diagnostic testing is initiated by the clinical scenario; however, *26-38% of patients with high-probability ventilation-perfusion (VQ) scans in the setting of known DVT are asymptomatic*^{4,5} Clinical estimates of the probability of PE are clearly not sufficient for individual patient management decisions.

The second reason for imprecision is that the widely used tests and algorithms for suspected venous thromboembolism (which includes both DVT and PE) are limited in accuracy and inconsistently applied. The ideal diagnostic test should be accurate, direct (objective), rapid, safe, readily available, and of reasonable cost. *Only approximately 30% of patients (probably much less in the current medicolegal climate) with clinically suspected PE have the disease.*⁶ Therefore, a test able to provide information regarding the presence and significance of other chest disease would also be desirable. None of the common tests in use (other than CT) meet all or even most of these criteria.

The use of CT in the assessment of patients with possible thromboembolic disease has coincided with the development of rapid helical (spiral) scanners, which enable angiogram-like images of the pulmonary circulation in a single breath-hold. This technique has revolutionized the approach to the patient with possible PE and offers significant and important improvements over the traditional diagnostic approach (chest radiograph and VQ scan) in the initial assessment of these patients. New scanners acquire

four channels of data simultaneously (hence the name “quad scanner”) and faster (8 and possibly 16 channels) scanners are in development. These multi-channel scanners have significant advantages over single channel helical CT; these will be outlined and illustrated after a brief review of pertinent issues in pulmonary CT angiography. ***There is no question that multi-channel CT (MCCT) is the new gold standard in the diagnosis of PE and it is unethical to perform randomized trials that exclude some patients from MCCT.***

Single Channel Helical CT Angiography

All published literature in CT pulmonary angiography refers to studies obtained with single channel helical CT, and a basic understanding of this information is essential to an understanding of the significant impact of multi-channel scanning in this setting. All helical data sets are volumetric and permit image reconstructions at overlapping intervals, improving density discrimination between small adjacent structures of different attenuation (such as thrombi within enhancing arteries). The central thorax can also be scanned in a single breath hold (no respiratory motion) on these scanners; these features in concert enable high quality multiplanar reconstructions. Helical pulmonary CT angiography has become the method of choice in the assessment of patients with suspected venous thromboembolism even prior to the development of multi-channel technology.

With single channel scanners, we use a collimation of 3 mm and a reconstruction interval of 2 mm after acquiring data from the top of the aortic arch to the level of the inferior pulmonary veins (or lower depending on the breath hold) during a single 20-25 second breath-hold. If necessary, scans can be performed during either quiet respiration or two distinct breath-holds separated by a short (5-10 seconds) interval although this introduces motion and limits assessment of smaller, peripheral vessels. Few patients have difficulty tolerating the examination. We use 100-150 cc of low osmolar, nonionic contrast (30-48% iodine) injected at a rate of 2.5-3 cc/sec. Optimal opacification of the pulmonary vasculature is achieved through the use of a “timing run” or by using the Smart Prep (General Electric Medical Systems, Milwaukee) program. This “timing run” facilitates optimal pulmonary arterial opacification and also serves as a check on the quality of the study to follow; scanning technique may require alteration if the preliminary images show poor vascular opacification. Occasionally, central thrombi can be identified even on the “timing run.”

The thinly-collimated overlapping images permit detailed assessment of the central airways, hilar and mediastinal lymph nodes, and of the lungs and pleural surfaces. This ancillary information is not provided by any other diagnostic test commonly used in the assessment of patients with suspected venous thromboembolism and is of importance in the symptomatic patient with an unknown diagnosis.

CT, like pulmonary angiography, directly depicts thrombi within the opacified arterial lumen as intravascular filling defects surrounded by a rim of contrast material or as meniscus-like filling defects with contrast extending around the edges of the clot. ***A nonopacified artery is nondiagnostic unless the diameter of the vessel is clearly expanded.*** Lack of filling of small arteries is nondiagnostic at angiography as well; the ability of CT to depict and assess vascular diameter is an advantage of CT over angiography. Arteries peripheral to a central thrombus may or may not opacify; central clot does not necessarily completely obstruct the distal flow of contrast. Although nonocclusive clot is depicted by CT, false negative scintigraphy in this setting is well-known. The CT findings diagnostic of chronic PE are also modified from angiographic criteria and include mural thrombus (adherent to the arterial wall), webs, stenoses, or strictures of the arteries, and a central “dot” of contrast surrounded by circumferential thrombus indicative of recanalization. CT, like angiography, usually enables distinction between acute and chronic PE; this is not possible with scintigraphy.

Technical pitfalls in CT interpretation relate to the physical properties of contrast material, mechanics of contrast injection, image reconstruction algorithm, and miscellaneous factors such as respiratory motion. These are readily recognized by the experienced observer. However, even with a high quality examination, several common errors must be avoided. Pulmonary arterial vasoconstriction, which often occurs in areas of pleural or parenchymal disease, can result in vascular nonopacification due to slow blood flow in the area of abnormality. Pulmonary veins may also fail to opacify because scanning is performed during the arterial enhancement phase. Veins and arteries can be readily differentiated by experienced observers, but nonopacified vessels without caliber expansion should never be considered diagnostic of PE regardless of their nature. Periarterial abnormalities, such as lymph node enlargement or infiltration of the axial interstitium by edema fluid, inflammation, or neoplasm, can mimic eccentric or mural thrombus. Multiplanar reconstructions, easily performed in 10-15 minutes on standard workstations, are of particular diagnostic value in problematic cases. However,

reformatations cannot produce results better than the initial axial images from which they are generated; again, meticulous CT technique is essential.

“Accuracy” of Single Channel Helical CT Angiography

Studies of accuracy usually compare CT to pulmonary angiography, the favored “gold standard” in PE diagnosis. CT and angiography are both direct tests for PE which depict actual endovascular thrombi. The accuracy of CT, like that of angiography, depends on many variables, including the technical adequacy of the examination, the number and location of thrombi (extent of disease), prevalence of PE in the population, reader experience, and the criteria used for a positive or negative test result. CT accuracy also depends upon the actual accuracy of the “gold standard” and can therefore not exceed 100%. This is intuitive; however, clear CT diagnoses of PE can occur in the setting of normal or nondiagnostic angiograms.⁷ A simple quotation of the published sensitivity and specificity of CT is simplistic yet is routinely incorporated into lectures on this topic. *The accuracy of even single channel CT for PE is actually well over 100%!*

More relevant is the fact that properly performed CT and angiography depict identical information, but in different ways. Remy-Jardin and colleagues showed that the number of arteries depicted with properly performed CT through the segmental level is equivalent to that of angiography and that perfect anatomic correlation between the two modalities was present in 188 central emboli in 39 patients.⁷ Given the superior contrast resolution of CT and the elimination of overlapping structures due to the nature of cross sectional imaging, it is not surprising that *single channel CT angiography is a least as good as and should be better than cut-film-based pulmonary angiography* in most respects. Both studies are limited in the display of subsegmental arteries due to their small size. Conventional angiographic dual observer agreement is only slightly better than random guessing at the subsegmental level (66%) and falls to 13% with three readers.^{6,8} This is of controversial significance, however, for in patients without concomitant cardiopulmonary disease, no difference in the incidence of recurrent PE between treated and untreated patients has been noted.⁹ However, in patients with limited cardiopulmonary reserve, such small emboli may be fatal. The residual DVT burden is of major importance in this setting, as this determines the risk of continued or recurrent thromboembolism. *Assessment of the deep venous system can be performed at the same sitting as the single channel chest CT.*

Scintigraphy: An Indirect Test (or Educated Guess)

The VQ scan depicts neither thrombus nor the actual pulmonary circulation; it is an indirect test, and the presence or absence of PE is based on inference. In a study of 185 perfusion defects in 68 patients, only 16% corresponded to visible angiographic abnormalities; only 10 of 35 segmental or larger scintigraphic mismatches corresponded to angiographically proven emboli, while 43 segmental thrombi identified at angiography had no evident ventilation-perfusion mismatches.¹⁰

Patients with proven PE in the setting of low-probability scans do not necessarily have subsegmental or a few small emboli; central thrombus involving main or lobar arteries is more frequent than isolated subsegmental thrombi (31% to 17%) in these patients.¹¹ False positive scintigraphy (high probability scans in the absence of PE) also occur; 12% of such patients may have normal angiograms.⁶ Clearly, low- or indeterminate probability scans do not constitute sufficient evidence upon which to base treatment decisions, particularly in patients with other cardiopulmonary disease.

The problems with false negative, false positive, and indeterminate examinations exist even if the scintigraphic study is of highest quality because it is an indirect test. Due to its inferential nature, scintigraphy is also unable to depict other potentially important pathology in the chest. Recent studies have directly compared single channel CT to scintigraphy in the setting of possible PE. Cross and colleagues found that CT enabled confident diagnosis (positive, negative, or alternative) in 90% of patients compared to 54% for scintigraphy.¹² CT also detected thrombi missed or considered indeterminate at scintigraphy, although the opposite did not occur. A unique study conducted by van Rossum and colleagues evaluated 123 patients who underwent both VQ and CT within a 48 hour period; each patient was assessed twice by a radiologist and a pulmonologist with associated clinical information, chest radiographs, and either the VQ scan or the CT.¹³ There was a significant difference in the number of inconclusive evaluations with scintigraphy (28%) in comparison to CT (8%). CT also had a higher sensitivity (75% to 49%) and specificity (90% to 74%) for PE than did scintigraphy, and enabled twice the number of alternative diagnoses (93% to 51%). Of note, these alternative diagnoses excluded conditions evident on the chest radiograph, but included entities such as aortic dissection, mediastinitis, and malignancy. In the 35 indeterminate scintigrams, CT correctly identified the final diagnosis

in 29 (13 PE, 11 alternative, 5 normal). These authors suggested that CT replace the VQ scan.

Routine scintigraphy should be discontinued, particularly in patients with either abnormal chest radiographs or concomitant cardiopulmonary disease; such patients have a rate of indeterminate scintigraphy that is unacceptably high and also often benefit from the pleuroparenchymal assessment possible even with single channel CT. Imaging of the venous system is an important part of the diagnostic assessment of these patients and should follow the chest CT.

Multi-channel CT: The Definitive Test

The advantage of multi-channel CT is speed. The GE LiteSpeed scanner, for example, is 8-times faster than a single channel scanner in identical volume coverage. Thus, much larger volumes can be covered with the same collimation as a single slice scanner; alternatively, a similar volume can be covered with much thinner collimation. In practice, we use 1.25mm collimation, single breath hold, HS mode (pitch=6), and cover the entire chest in one breath hold. ***Therefore, we get both thinner sections (better resolution) and a larger coverage area than with single channel scanning.*** This facilitates depiction of smaller peripheral vessels, increases the resolution and quality of multiplanar reformations, and leads to potential applications of dynamic repeated acquisitions through questionable areas if necessary. We assess the pelvic and upper leg veins routinely with 10mm and 5mm collimation, respectively, 2-3 minutes after the start of the contrast injection. ***Tube cooling, often problematic in single channel scanning, does not limit multi-channel acquisitions.***

Image processing is an area of active research. Cardiac gating software is now available for multi-channel scanners that facilitates data acquisition only during quiescent phases of the cardiac cycle as well. Huge data sets, gated, with 1.25mm overlapping reconstructions can be sent to powerful computers; software engineers (including the Emory-Georgia Tech Division of Biomedical Engineering) in concert with radiologists are only beginning to develop new means of processing this information to extract pertinent diagnostic value with the click of a mouse. Axial images will probably be only a small part of CT display in the not-so-distant future.

In sum, single channel CT is (was) the test of choice for patients with suspected PE. Multi-channel CT, however, represents a major advance in our ability to scan large volumes rapidly with collimation sufficiently small to resolve small vessels. ***Image processing represents the future- invest in medical software research now!***

REFERENCES

1. Siddique RM, Siddique MI, Rimm AA. Trends in pulmonary embolism mortality in the US elderly population: 1984 through 1991. *Am J Public Health* 1998; 88(3):478-480.
2. Goldhaber SZ, Hennekens CH, Evans DA, et al. Factors associated with the correct antemortem diagnosis of major pulmonary embolism. *Am J Med* 1982; 73:822-826.
3. Proctor MC, Greenfield LJ. Pulmonary embolism: diagnosis, incidence, and implications. *Cardiovasc Surg* 1997; 5(1):77-81.
4. Monreal M, Ruiz J, Olazabal A, Arias A, Roca J. Deep venous thrombosis and the risk of pulmonary embolism: a systematic study. *Chest* 1992; 102:667-681.
5. Decousus H, Leizorovicz A, Parent F, et al. A clinical trial of vena cava filters in the prevention of pulmonary embolism in patients with proximal deep venous thrombosis. *N Engl J Med* 1998; 338:409-415.
6. The PIOPED investigators. Value of the ventilation/perfusion scan in acute pulmonary embolism: results of the Prospective Investigation of Pulmonary Embolism Diagnosis (PIOPED). *JAMA* 1990; 263:2753-2759.
7. Remy-Jardin M, Remy J, Deschildre F. Diagnosis of pulmonary embolism with spiral CT: comparison with pulmonary angiography and scintigraphy. *Radiology* 1996; 200:699-706.
8. Quinn MF, Lundell CJ, Klotz TA, et al. Reliability of selective pulmonary arteriography in the diagnosis of pulmonary embolism. *AJR* 1987; 149:469-471.
9. Stein PD, Henry JW, Relyea B. Untreated patients with pulmonary embolism: outcome, clinical, and laboratory assessment. *Chest* 1995; 107:931-935.
10. Breslaw BH, Dorfman GS. Ventilation/perfusion scanning for prediction of the location of pulmonary emboli: correlation with pulmonary angiographic findings. *Radiology* 1992; 185:180-185.
11. Stein PD, Henry JW. Prevalence of acute pulmonary embolism in central and subsegmental pulmonary arteries and relation to probability interpretation of ventilation/perfusion lung scans. *Chest* 1997; 111:1246-1248.
12. Cross JLL, Kemp PM, Walsh CG, Flower CDR, Dixon AK. A randomized trial of spiral CT and ventilation perfusion scintigraphy for the diagnosis of pulmonary embolism. *Clin Radiol* 1998; 53:177-182.
13. van Rossum AB, Pattynama PMT, Mallens WMC, Hermans J, Heijerman HGM. Can helical CT replace scintigraphy in the diagnostic process in suspected pulmonary embolism? A retrospective-prospective cohort study focusing on total diagnostic yield. *Eur Radiol* 1998; 8:90-96.

Interventional Chest Radiology

Cristopher A. Meyer, MD



There are numerous excellent reviews of transthoracic needle aspiration biopsy (1,2,3). This workshop will discuss the mechanics of this procedure, some problem solving techniques for difficult biopsies, the common procedural complications and management of these complications.

Preoperative Evaluation

Common indications for TTNA biopsies include: solitary pulmonary nodules, focal opacities that do not clear with antibiotics, proof of first metastases in a patient with a known primary malignancy and focal abnormalities in immunosuppressed patients (4,5). The only absolute contraindication to biopsy is the inability to cooperate with instructions, particularly to suspend respirations, unless the mass is large. Relative contraindications include bleeding diatheses (INR > 1.3), platelets less than 100,000/ml, severe pulmonary hypertension, prior pneumonectomy or FEV1 less than 1 liter. Hemorrhagic complications are more common in patients on aspirin or in renal failure as platelet function is the primary determinant of bleeding complications. Patients should suspend aspirin 1 week prior to the procedure. In the case of chronic renal failure, desmopressin (DDAVP) 0.3 ug/kg may be administered intravenously 30 to 60 minutes prior to the procedure (6).

The patient should be informed of all common complications. This should include a pneumothorax rate of 20-30% (in patients with severe emphysema this may be as high as 50%). Approximately 10-15% of patients may require chest tubes and we obtain consent for chest tube placement prior to the procedure to avoid any issues related to conscious sedation. Bleeding occurs in up to 5% of patients and the possibility of hemoptysis should be specifically discussed with patients as they find this the most distressing of all the complications. No case of infection from TTNA biopsy has been reported. Death occurs in 1 in 10,000 biopsy procedures due to air embolism or hemorrhage. Other topics you may choose to review in the consent procedure include a nondiagnostic sample, malignant seeding of the needle track, and drug allergies to conscious sedation.

Technique

Many modalities are currently available to the radiologist for TTNA biopsy including: fluoroscopy, ultrasound, CT, or CT fluoroscopy (7,8,9). Fluoroscopy is generally reserved for larger lesions that are

readily visible while ultrasound is useful for peripheral lesions that abut the pleura. Both have the advantage of real time needle placement as does CT fluoroscopy. Choice of modality is most often based on local equipment availability and operator preference.

We perform the majority of our biopsies using CT fluoroscopy in the interrupted real time mode. Incremental needle advancement is performed followed by a series of quick "looks" to determine adequacy of the trajectory. While this does not take advantage of the real time capabilities of the unit, it allows a more controlled environment for instructing residents and results in lower fluoroscopy times and thus, radiation dose. Real time needle placement can be performed if the target to be sampled is adjacent to vital structures.

Patients receive local anesthesia 1% Xylocaine buffered with 8.4% Sodium bicarbonate solution (9:1 ratio). In addition, liberal use of conscious sedation is recommended particularly in anxious patients (10). We titrate doses of Midazolam (0.5-1 mg increments) and Fentanyl (50 ug increments) to achieve a patient who is relaxed and cooperative. Midazolam also has amnestic properties. All patients receiving conscious sedation should be monitored by a nurse or trained personnel and vital signs (pulse, blood pressure and peripheral oxygen saturation) recorded.

Choice of biopsy needles is generally based on personal preference (11). There is no difference in pneumothorax rates in needle gauges ranging from 18-25g. Multiple systems currently exist for fine needle aspiration biopsy. In general, one should choose a system that does not limit your options if you decide to switch to a larger gauge needle or to perform core biopsies. The system we use currently has a 19g diamond point thin walled trocar/introducer needle. This will accommodate a 22g or 20g Chiba needle, a 20g Franseen needle or a 20g spring loaded core biopsy needle, all calibrated to have a 17mm throw beyond the end of the introducer needle.

The biopsy proceeds as follows: 1. Find the best transthoracic approach to the nodule. The importance of this step should not be underestimated. The goal will be the shortest approach with the least angulation, crossing the minimum number of pleural surfaces with the patient in the most comfortable position to minimize movement. In general, supine or prone positioning is preferable to either decubitus position. Arms down at the side is generally better tolerated by older patients than arms extended over the head. If there are multiple lesions, smaller lesions in

the apices may be preferable to larger lesions at the lung bases as they will move less with respiration. 2. The entry site is confirmed using a quick localizing image of a metallic marker. Don't hesitate to move your marker if you are not completely satisfied with its position. It is much easier to start with the correct entry site than to try to adjust for a poor choice. 3. The skin is sterilely prepped and draped. Buffered lidocaine is infused in the subcutaneous tissues for local anesthesia. 4. A second image is obtained with the anesthesia needle in place to confirm an accurate approach to the target. 5. The 19g trocar needle replaces the anesthesia needle in the track to a position just outside the pleura. Another image is obtained to confirm that this needle is on target. Additional local anesthesia is administered just outside the pleura. 6. The needle is advanced into the lesion. All imaging and needle placements should be performed with the patient in the same phase of suspended respiration.

The sensitivity of TTNA biopsy for nodules exceeding 1 cm should be approximately 95% for malignancy while benign diagnoses are more problematic with accuracies ranging from 16 to 91%. Core needle biopsies have resulted in improved yields for benign disease (12). On-site cytopathology support is essential in improving diagnostic yield (13).

In accessing difficult lesions it is useful to be aware of several additional maneuvers (14). It may be preferable to approach a lesion at an angle other than perpendicular to the "Z" axis. The CT gantries can be angled 15-20 degrees in a cranial or caudal dimension. By angling the gantry, the path of the needle can be visualized without the need to mentally extrapolate over multiple axial sections (15). With real time CT fluoroscopy, small lesions may be positioned under the needle tip while the needle is extrapleural. Under fluoroscopic observation, the patient is instructed to suspend respiration when the nodule moves into position under the needle. Accessing masses without traversing the pleura eliminates the possibility of a pneumothorax. Creative approaches to central masses via extrapleural paths include the use of a preexisting pleural fluid collections, extrapleural paraspinal pathways (16), extrapleural saline window (17,18) or transosseous needle placement (19,20).

Following the procedure we obtain an immediate PA chest radiograph and observe the patient in a recovery area for 1 hour. A second radiograph is obtained at the end of the first hour. If both radiographs are stable and the patient is asymptomatic, they change into street clothes and are allowed to ambulate for 2 or 3 more hours and return for a final chest radiograph 4 hours post procedure prior to discharge.

Complications

There are several well recognized complications associated with TTNA biopsy (21). Pneumothorax is the most common complication of transthoracic needle aspiration biopsy and occurs in 20-30% of cases. Autologous blood patch and post procedure biopsy site dependent positioning may reduce the incidence of pneumothoraces (22). While most pneumothoraces are small and asymptomatic, enlarging or symptomatic ones require small bore pleural catheter management (23,24). We currently admit all our patients for a 23 hour "short stay" observation while managing the chest tube. Other authors have suggested a more aggressive approach to catheter management to include outpatient catheter management (25,26,27). This should be based on local access to healthcare facilities.

Hemoptysis is an alarming although almost always self-limited complication of needle biopsy that occurs in 5% of patients. While fatalities are rare, bleeding is the most commonly reported cause of death from lung biopsies (1). In our experience, bleeding is more common with the Franseen needle than the Chiba needle, although the tissue samples are generally better. The initial treatment for massive hemoptysis is placing the biopsy site down to avoid contaminating the contralateral lung. If severe bleeding continues, bronchial embolization, balloon occlusion of a segmental bronchus or surgical resection are the remaining treatment options.

Air embolism is fortunately a rare complication of TTNA procedures. The mechanism is air entry into a pulmonary vein via the needle or a bronchoalveolar venous fistula. Treatment includes left lateral decubitus positioning, supplemental oxygen and hyperbaric therapy. Air embolism is often a fatal complication of TTNA and occurs in approximately 1 in 10,000 procedures.

Needle tract malignant contamination has been reported experimentally in up to 60% of cases (28,29). It is unclear whether cellular contamination will eventually result in mature tumor masses. Currently the long term survival for lung cancer is poor and thus the impact of needle tract contamination is less relevant. As more Stage I lesions are diagnosed and biopsied, this issue will require further investigation.

SELECTED READING

1. Moore EH. Technical aspects of needle aspiration lung biopsy: a personal perspective. *Radiology* 1998; 208: 303-318.
2. Klein JS, Zarka MA. Transthoracic needle biopsy: an overview. *J Thorac Imaging* 1997; 12: 232-249.
3. Gunther RW. Percutaneous interventions in the thorax. *JVIR* 1992; 3: 379-390.

4. Conces DJ, Clark SA, Tarver RD and GR Schwenk. Transthoracic aspiration needle biopsy: value in the diagnosis of pulmonary infections. *AJR* 1989; 152: 31-34.
5. Tarver RD and DJ Conces. Interventional chest radiology. *Radiologic Clinics of North America* 1994 32(4): 689-709.
6. Mannucci PM. Desmopressin (DDAVP) in the treatment of bleeding disorders: the first 20 years. *J of Am Soc of Hematology* 1997; 90: 2515-2521.
7. Carswell H. Image guidance assists needle biopsy of thorax. *Diagnostic Imaging* 1992: 143-145.
8. Gardner D, vanSonenberg E, D'Agostino HB, Casola G, Taggart S and S May. CT-guided transthoracic needle biopsy. *Cardiovasc Intervent Radiol* 1991; 14: 17-23.
9. Yang PC. Ultrasound-guided transthoracic biopsy of peripheral lung, pleural and chest-wall lesions. *J Thorac Imaging* 1997; 12: 272-284.
10. Hurlbert BJ, Landers DF. Sedation and analgesia for interventional radiologic procedures in adults. *Seminars in Interventional Radiology* 1987; 4: 151-160.
11. Dahmert WF, Hoagland MH, Hamper UM, Erozan YS, Pierce JC. Fine needle aspiration biopsy of abdominal lesions: diagnostic yield for different needle tip configurations. *Radiology* 1992; 185: 263-268.
12. Boiselle PM, Shepard JO, Mark EJ, Szyfelbein WM, Fan CM, Slanetz PJ, Trotman-Dickenson B, Halpern EF, McLoud TC. Routine addition of an automated biopsy device to fine-needle aspiration of the lung: a prospective assessment. *AJR* 1997; 169: 661-666.
13. Austin JHM, Cohen MB. Value of having a cytopathologist present during percutaneous fine-needle aspiration biopsy of lung: report of 55 cancer patients and metaanalysis of the literature. *AJR* 1993; 160: 175-177.
14. Yankelevitz DF, Vazquez M, Henschke CI. Special techniques in transthoracic needle biopsy of pulmonary nodules. *RCNA* 2000; 38: 267-279.
15. Stern EJ, Webb WR, Gamsu G. CT gantry tilt: utility in transthoracic fine-needle aspiration biopsy. *Radiology* 1993; 187: 873-874.
16. Grant TH, Stull MA, Kandallu K, Chambliss JF. Percutaneous needle biopsy of mediastinal masses using a computed tomography-guided extrapleural approach. *J Thorac Imaging* 1998; 14-19.
17. Langen HJ, Klose KC, Keulers P, Adam G, Jochims M, Gunther RW. Artificial widening of the mediastinum to gain access for extrapleural biopsy: clinical results. *Radiology* 1995; 196: 703-706.
18. Moulton JS. Artificial extrapleural window for mediastinal biopsy. *JVIR* 1993; 4: 825-829.
19. Glynn TP. Transosseous approach for thoracic needle biopsy. *Radiology* 1990; 177: 278-279.
20. D'Agostino HB, Sanchez RB, O'laoide RM, Oglevie S, Donaldson JS, Russack V, Villaveiran RG and E vanSonnenberg. Anterior mediastinal lesions: transsternal biopsy with CT guidance. *Radiology* 1993; 189: 703-705.
21. Shepard JO. Complications of Percutaneous Needle Aspiration Biopsy of the Chest, Prevention and Management. *Seminars in Interventional Radiology* 1994; 11: 181-186.
22. Moore EH. Needle -aspiration lung biopsy: a comprehensive approach to complication reduction. *J Thorac Imaging* 1997; 12: 259-271.
23. Laoide RO, Fundell LJ, vanSonnenberg E, D'Agostino H, Oglevie SB, Rosenkrantz H. Treatment of postbiopsy pneumothorax with a self-contained pneumothorax treatment device. *Radiology* 1994; 193: 393-395.
24. Casola G, vanSonnenberg E, Keightley A, Ho M, Withers C, Lee AS. Pneumothorax: radiologic treatment with small catheters. *Radiology* 1988; 166: 89-91.
25. Brown KT, Brody LA, Getrajdman GI, Napp TE. Outpatient treatment of iatrogenic pneumothorax after needle biopsy. *Radiology* 1997; 205: 249-252.
26. Gurley MB, Richli WR, Waugh KA. Outpatient management of pneumothorax after fine needle aspiration: economic advantages for the hospital and patient. *Radiology* 1998; 209: 717-722.
27. Yankelevitz DF, Davis SD, Henschke CI. Aspiration of a large pneumothorax resulting from transthoracic needle biopsy. *Radiology* 1996; 200: 695-697.
28. Ayar D, Golla B Lee JY, Nath H. Needletrack metastasis after transthoracic needle biopsy. *J Thorac Imaging* 1998; 13: 2-6.
29. Sawabata N, Ohta M, Maeda H. Fine-needle aspiration cytologic technique for lung cancer has a high potential of malignant cell spread through the tract. *Chest* 2000; 118: 936-939.

Tricks of the Trade: Reading CXRs and CTs on a Workstation

David K. Shelton, Jr, MD

At the time of publication, no abstract was available.

Disclosure Statement: We use PACS equipment but don't have research or grant support.

Congenital Pulmonary Vascular Anomalies: The Ins and Outs

Laura E. Heyneman, MD

Objectives

To discuss arterial and venous pulmonary vascular anomalies, with particular attention to their radiologic appearance and clinical significance. Due to time limitations, topics will include some but not all of the following entities.

Arterial Anomalies

Absence of the main pulmonary artery: Two anatomic patterns predominate. In one type, there is an atretic main pulmonary artery, but the right and left pulmonary arteries persist; the pulmonary arteries receive blood flow via a patent ductus arteriosus (PDA). This pattern tends to present after birth, when the patent ductus arteriosus closes, leaving the bronchial arteries as the sole pulmonary blood supply. As the bronchial arteries are small and not functioning well as collaterals at birth, closure of the PDA leads to severe hypoxemia. The second type of absence of the main pulmonary artery is a truncus arteriosus, in which there is no anatomic remnant of the main pulmonary artery. Pulmonary blood flow is derived from a single great vessel that gives rise to both the aorta and pulmonary artery. Aortic arch anomalies are common, with a right arch present in approximately 40% of cases of truncus, and an interrupted arch in 20%. VSD's are frequent associations, and are invariably present in cases of truncus arteriosus. The chest radiograph demonstrates increased pulmonary vascularity (shunt vascularity) and enlargement of the cardiopericardial silhouette, with biventricular enlargement. MRI may provide a helpful adjunct to angiography and echocardiography. Features that are important to ascertain include the presence of associated VSDs and pulmonary arterial stenoses, the presence of aortic interruption, the anatomy of the coronary circulation (particularly in truncus arteriosus, where a single coronary artery is present in approximately 15% of cases), and the relationship of the truncal valve to the mitral and tricuspid valves.

Proximal interruption of the pulmonary artery: The hilar pulmonary artery is atretic, but the vessels in the lung are patent. Blood supply to the vasculature distal to the stenosis is supplied by bronchial collaterals or a PDA. Interruption of the right pulmonary artery is much more common than interruption of the left. Proximal interruption of the

right pulmonary artery is associated with pulmonary arterial hypertension, and proximal interruption of the left pulmonary artery is associated with congenital heart disease, particularly tetralogy of Fallot. Patients with proximal interruption of the right pulmonary artery may be asymptomatic and present incidentally, or may develop pulmonary arterial hypertension either as children or adults. Patients with proximal interruption of the left pulmonary artery usually present in infancy due to the associated congenital heart disease. Patients may also present with hemoptysis due to the massive bronchial collaterals. Radiographs reveal a small affected lung and hilum, and the lung may be hyperlucent. The contralateral hilum is enlarged. There may be rib notching and pleural thickening from intercostal and transpleural collaterals. Contrast-enhanced CT reveals an absent proximal artery and patent small intrapulmonary arteries. The bronchial tree is normal. No air trapping is present with expiration, a finding that helps distinguish this entity from Swyer-James syndrome, with which it may be confused.

Pulmonary sling: In this entity, the left pulmonary artery arises anomalously off the right pulmonary artery. The aberrant left pulmonary artery passes to the right of the trachea and right mainstem bronchus, and then takes an abrupt left turn to pass between the trachea and the esophagus on its way to the left lung. The apposition of the aberrant left pulmonary artery and the right mainstem bronchus and trachea are responsible for the airway obstruction for which most patients present as infants. Lateral chest radiographs reveal anterior deviation of the distal trachea or mainstem bronchi, as well as absence of the posterior wall of the bronchus intermedius. Barium esophagrams demonstrate a mass impressing on the anterior wall of the esophagus. Both CT and MRI are diagnostic, and demonstrate the aberrant left pulmonary artery coursing through the mediastinum towards the left lung. There is a strong association with tracheobronchial anomalies, including incomplete septations of tracheal cartilage that result in a tracheal stenosis (the so-called ring/sling complex). The tracheal stenosis may cause significant respiratory distress that is completely separate from the vascular sling.

Pulmonary arterial stenosis: Stenoses may affect any portion of the pulmonary artery, from the level of the pulmonic valve to the distal, peripheral branches.

In patients with pulmonic valvular stenosis, the jet of blood which flows through the stenotic valve is directed through the main pulmonary artery into the left pulmonary artery. The result is post-stenotic dilatation of the main and left pulmonary arteries, with the right pulmonary artery being of normal size. Peripheral pulmonary arterial stenoses may be multiple and bilateral. The chest radiograph most often demonstrates small nodular opacities within the lungs which correspond to foci of post-stenotic dilatation. Other radiographic findings include enlargement of the right heart and central pulmonary arteries secondary to cor pulmonale or regional hyperlucency from oligemia. Associations with peripheral pulmonary arterial stenoses include congenital rubella infection, Williams syndrome (hypercalcemia, mental retardation, elfin facies, supra-valvular and peripheral pulmonic arterial stenoses as well as stenoses of other vessels), congenital heart disease (particularly tetralogy of Fallot) and Ehlers-Danlos syndrome.

Venous Anomalies

Unilateral pulmonary venous atresia: Congenital unilateral pulmonary venous atresia is a rare condition which usually presents in infancy due to associated congenital heart disease, or may present in childhood or early adulthood with hemoptysis or recurrent infections. The atresia is usually limited to the veno-atrial junction. Chest radiographs reveal a small ipsilateral hemithorax and hilum, as well as reticular opacities and Kerley B lines within the lungs. We have recently described the CT findings in 3 adults with unilateral venous atresia (in press). The left atrial wall is smooth in the expected location of the pulmonary veins. Extensive pulmonic-to-systemic venous collaterals may result in increased mediastinal soft tissue which may simulate an infiltrative process such as fibrosing mediastinitis. The diagnosis is suggested on MRI or angiography by the presence of retrograde flow within the ipsilateral pulmonary artery due to systemic-to-pulmonic collaterals. Definitive diagnosis is dependent on the angiographic demonstration of absent pulmonary veins on levophase imaging or nonopacification of the veins on capillary wedge angiography.

Anomalous pulmonary venous return: Anomalous pulmonary venous return refers to a form of a left-to-right shunt, in which blood from the lungs enters into the right heart or systemic veins rather than the left atrium. Anomalous pulmonary venous return may be total or partial. Total anomalous pulmonary venous return usually presents in infancy either due to cyanosis from necessary admixture through an atrial septal defect or due to venous obstruction, whereas partial anomalous pulmonary venous return may be diagnosed incidentally or due to symptoms

from other associated cardiovascular anomalies (particularly a sinus venosus atrial septal defect, which is present in approximately 85%). Total anomalous pulmonary venous return occurs in four forms: 1.) a supracardiac form, in which the anomalous vessel connects to a vena cava; 2.) a cardiac form, in which the anomalous vessel connects directly to the right atrium or the coronary sinus; 3.) an infracardiac/infradiaphragmatic form, in which the anomalous vessel courses through the esophageal hiatus and connects to a systemic vein, usually the portal vein; 4.) a mixed form (the least common of the four). The infradiaphragmatic form is always associated with venous obstruction, partially as a result of intrinsic stenosis of the anomalous vessel and partially due to the fact that the entire pulmonary blood flow has to course through the hepatic sinusoids. Partial anomalous pulmonary venous return is more common than the total form, and occurs 2 to 10 times more commonly on the right than the left. In partial anomalous pulmonary venous return, the anomalous vein usually connects to the nearest adjacent systemic vein or to the right atrium. For example, the right upper lobe pulmonary vein most often connects directly to the superior vena cava. The chest radiograph in partial anomalous pulmonary venous return is normal when the pulmonary-to-systemic flow ratio is less than 2:1. The anomalous vessel may also be radiographically apparent, particularly in the lower lobes. Hypogenetic lung syndrome (scimitar syndrome) is a form of partial anomalous pulmonary venous return which is discussed separately (*see below*).

Venous varix: Varicosities of the pulmonary veins are often acquired lesions, associated with mitral valvular disease. However, congenital pulmonary varicosities do exist. The lesions consist of abnormally dilated and tortuous pulmonary veins, usually just before their attachment to the left atrium. On the right, the inferior pulmonary vein near the medial basilar segment is usually affected, whereas the lingular vein is most often involved on the left. They are usually discovered incidentally as round or oval homogeneous opacities in the medial third of the lungs. The diagnosis is easily made on contrast-enhanced CT or MRI.

Anomalies Affecting Both Arteries and Veins

Hypogenetic lung syndrome (scimitar syndrome): Hypogenetic lung syndrome is characterized by a constellation of findings that include: partial anomalous pulmonary venous return from the right lung, a hypoplastic right lung and right pulmonary artery, and systemic arterial supply to the right lung (usually the right lower lobe). The term scimitar syndrome refers to the shape of the anomalous pulmonary vein; the vein is gently curved as it courses inferiorly

within the right lung, and thus resembles the shape of a Turkish sword, or scimitar. The vein usually drains into the inferior vena cava below the right hemidiaphragm. Other abnormalities associated with the syndrome include bronchiectasis, mirror image bronchial anatomy (usually bilateral bilobed lungs), duplicated diaphragm, and cardiovascular anomalies. Of note, whereas there is a very strong association between other forms of partial anomalous pulmonary venous return and sinus venosus atrial septal defects, only approximately 15% of patients with scimitar syndrome have a sinus venosus ASD.

Pulmonary arteriovenous malformations (AVM):

A pulmonary arteriovenous malformation is an abnormal communication between one or more pulmonary arteries and pulmonary veins. The lesions usually present in the third decade of life with hemoptysis, paradoxical emboli, cyanosis, or orthodeoxia. There is a strong association with Osler-Weber-Rendu; 60-90% of patients with pulmonary AVMs have the disease, and 15% of patients with Osler-Weber-Rendu have pulmonary AVMs. AVMs most commonly appear as a lobulated parenchymal mass with a large feeding artery and draining vein. They are more common in the lower lobes than the upper lobes, and are multiple in one-third of cases. Diagnosis may be made on CT, which delineates the feeding artery and draining vein communicating with a well circumscribed homogeneous nodule. Volumetric spiral CT is helpful in depicting the lesions via multiplanar reformations as well as maximum intensity projection (MIP) reconstructions. However, most patients undergo pulmonary angiography to confirm the diagnosis and to treat larger lesions with coil embolization.

Systemic Supply to the Lungs

Bronchopulmonary sequestration: A bronchopulmonary sequestration is a congenital abnormality in which a portion of the lung parenchyma is separated from the tracheobronchial tree and is supplied by a systemic artery. There are two forms: 1.) an intralobar variety, which accounts for 75% of sequestrations, and which is contained by the same visceral pleura as the remainder of the lung 2.) an extralobar variety which is contained by its own visceral pleural envelope. Both types of sequestration are more common within the lower lobes, left greater than right. Intralobar sequestrations usually present with recurrent infections, whereas extralobar sequestrations themselves are usually asymptomatic, but are discovered incidentally during the work-up of one of the other congenital anomalies with which they are associated (such as diaphragmatic hernias and congenital heart disease). Radiographic findings include a persistent opacity, either homogeneous or heterogeneous, within a posteromedial lower lobe.

Occasionally, a tubular opacity representing a focus of mucoid impaction or the aberrant systemic artery will be radiographically evident. On CT, the parenchyma within the sequestration is abnormal, and may demonstrate consolidation, cysts, regions of air trapping, or all of the above. Contrast-enhanced CT may be required to delineate the aberrant systemic vessel. Some investigators have suggested that intralobar sequestrations may be acquired rather than congenital abnormalities; they believe that the inciting event is an acquired focal bronchial obstruction, with subsequent parasitization and recruitment of adjacent systemic arteries to supply the abnormal lung. However, cases of intralobar sequestration have been reported in utero and at birth, and it is likely that at least some of the intralobar sequestrations are indeed congenital.

Systemic arterial supply to normal lung: This is a rare entity in which a systemic artery supplies otherwise normal lung; unlike in the case of bronchopulmonary sequestration, in this situation the parenchyma supplied by the systemic artery is normal and communicates normally with the tracheobronchial tree. The systemic artery usually replaces the normal pulmonary artery to the region supplied. The parenchyma is then drained by normal pulmonary veins. The left lower lobe is most often affected. Patients may present with hemoptysis or congestive heart failure due to the high pressure blood flow to a region of very low vascular resistance. Radiographs may depict the large systemic vessel as a tubular or oval opacity. The diagnosis may be made on CT when absence of the left lower lobe pulmonary artery is seen in conjunction with normal bronchial anatomy and a large systemic artery arising off the descending aorta.

REFERENCES

Developmental anomalies affecting the pulmonary vessels. In Fraser RS, Colman N, Muller NL, Pare PD: *Fraser and Pare's Diagnosis of Diseases of the Chest*, 4th edition. Philadelphia: WB Saunders, 1999, 637-675.

Ellis K. Developmental abnormalities in the systemic blood supply to the lungs. *AJR* 1991;156:669-79.

Harrison JK, Hearne SE, Baker WA, et al. Esophageal varices in association with unilateral pulmonary vein atresia. *Catheterization and cardiovascular diagnosis*. 1196;38:387-92.

Dillon EH, Camputaro C. Partial anomalous pulmonary venous drainage of the left upper lobe vs. duplication of the superior vena cava: Distinction based on CT findings. *AJR* 1993;160:375-9.

Woodring JH, Howard TA, Kanga JF. Congenital pulmonary venolobar syndrome revisited. *RadioGraphics* 1994;14:349-69.

Frazier AA, Rosado de Christenson ML, Stocker JT, et al. Intralobar sequestration: Radiologic-pathologic correlation. *RadioGraphics* 1997;17:725-45.

Miyake H, Hori Y, Takeoka H, et al. Systemic arterial supply to normal basal segments of the left lung: Characteristic features on chest radiography and CT. *AJR* 1998;171:387-92.

Lobar Atelectasis: Radiographic-CT Correlation

Kyung Soo Lee, MD

Department of Radiology, Samsung Medical Center,
Sungkyunkwan University School of Medicine, Seoul, Korea

Objective

The purpose of this workshop is to illustrate the spectrum of radiographic findings of lobar atelectasis and to correlate the radiographic findings with the CT findings.

Take-Home Points: The characteristic radiographic and CT findings of lobar atelectasis are well known. However, lobar atelectasis is a dynamic process, and atypical presentations may occur due to a number of different causes. After this workshop, the audience shall be familiar with radiographic and CT findings of

typical and atypical form of lobar atelectasis.

Right Upper Lobar Atelectasis

Right upper lobe (RUL) atelectasis results in overinflation of the right middle lobe and shift of the minor fissure superiorly and medially. It also results in compensatory overinflation of the right lower lobe (RLL) with shift of the major fissure anteriorly, superiorly and medially. The Golden's S sign denotes a centrally located mass with associated lobar atelectasis. The mass should be large enough to be borderforming with the adjacent hyperexpanded lung. With complete atelectasis, the RUL is either pancaked medially, simulating mediastinal widening or a mediastinal mass, or superiorly simulating an apical pleural cap.

On the lateral chest radiograph, an ill-defined opacity anterior to the trachea and obliteration of the anterior margin of the ascending aorta may sometimes be the only findings [1-3] (Fig. 1).

The minor fissure changes its position more dramatically than does the major fissure. With elevation of the minor fissure, the middle lobe shifts up laterally alongside the atelectatic upper lobe. On CT, the middle and upper lobes can be seen side-by-side anterior to the major fissure with the superior segment of the lower lobe posterior to the fissure. The major fissure maintains its previous contour, whether straight, concave, or convex [4-7].

Left Upper Lobar Atelectasis

With LUL atelectasis, the direction of movement is anterosuperior rather than directly superior as in

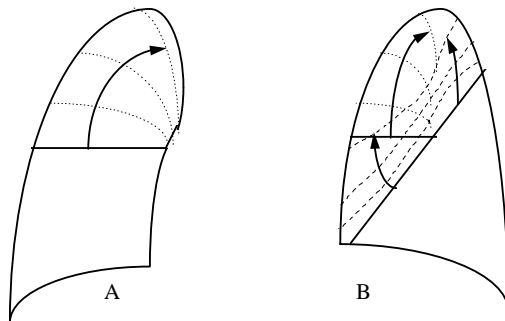


Fig.1. RUL atelectasis in progress

Table 1. Ancillary Radiographic Findings of Atelectasis of Right Upper Lobe

Fissural Reorientation	Elevated right minor fissure on PA radiograph, minor and major fissure marginate atelectatic lobe on lateral view
Hilum	Elevated to or above left hilum
Mediastinum	Tracheal deviation to ipsilateral side, mediastinal shift is less prominent than with lower lobe atelectasis
Diaphragm	Elevated, diaphragmatic tenting
Bronchus	Lateral position of bronchus intermedius on PA radiograph, larger lumen of RUL bronchus due to horizontal reorientation on lateral view

RUL atelectasis. The left pulmonary artery, which courses over the left main bronchus, restrains the bronchus and limits the superior migration of the atelectatic lobe [8]. For this reason, the superior segment of the LLL expands upward toward the apex of the left hemithorax. Therefore atelectasis of the left upper lobe is associated with increased opacity in the suprahilar region on the PA radiograph. As atelectasis progresses, it leads to increased opacity with poorly defined margins in the perihilar region.

On the lateral radiograph, the lateral portion of the major fissure is displaced forward and is placed tangentially resulting in a sharp interface (Fig. 2).

On CT scans, the atelectatic LUL forms a homogeneous opacity based on the anterior chest wall and the mediastinum. The posterior margin has a V-shaped contour from the lung apex to the hilum, where the apex of the V merges with the hilar vessels and bronchi. It is these hilar structures, which are relatively fixed in position, that tether the major fissure into the V-shape. The superior segment of the LLL is pulled forward along both the medial and lateral limbs of the V. The part of the superior segment that follows the medial limb forms a tongue of lung between the mediastinum and the atelectatic LUL. This tongue is visible on PA radiographs and has been called the Luftsichel (air-crescent) or periaortic lucency [7]. Less commonly, the major fissure may have a straight border rather than a V-shaped contour.

Occasionally the atelectatic lobe may have sharp margins on the PA radiograph simulating a hilar mass. With marked LUL atelectasis, the contour of the major fissure interface may appear continuous with that of the normal epipericardial fat on the lateral radiograph.

Right Middle Lobar Atelectasis

As the RML loses volume, the minor and major fissures move toward each other in an inferomedial and superomedial direction, respectively. The RML thus assumes an oblique orientation and on the PA

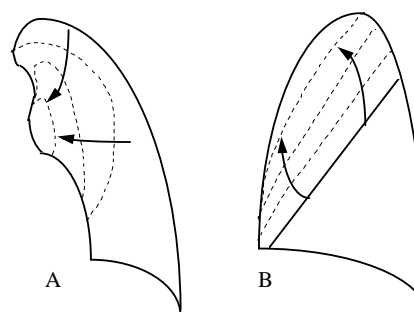


Fig.2. LUL atelectasis in progress

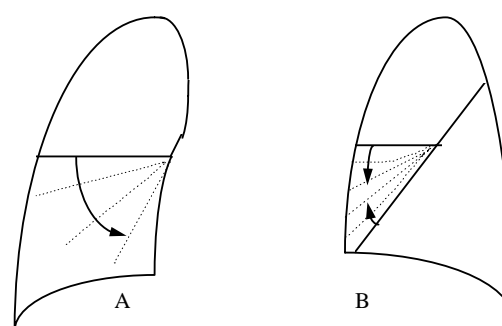


Fig.3. RML atelectasis in progress

radiograph results in a poorly defined increased opacity that obscures the right heart border. In general, the greater the atelectasis and the greater the reorientation of the RML, the more difficult it is to recognize the atelectasis on PA radiograph. On the lateral view, RML atelectasis is seen as a triangular opacity marginated superiorly by the minor fissure and inferiorly by the major fissure. The apex of the triangle is in the hilar area, and the base is located peripherally (Fig. 3).

Table 2. Ancillary Radiographic Findings of Atelectasis of Left Upper Lobe

Fissural Reorientation	Anterior displacement of major fissure on lateral radiograph
Hilum	Elevation of left hilum both on PA and lateral radiograph
Mediastinum	Anterior right lung herniation, producing prominent anterior margin of ascending aorta on lateral view
Diaphragm	Elevation with peak-like contour
Bronchus	Transverse orientation of left main bronchus resulting in enlarged orifice of LUL bronchus on lateral radiograph

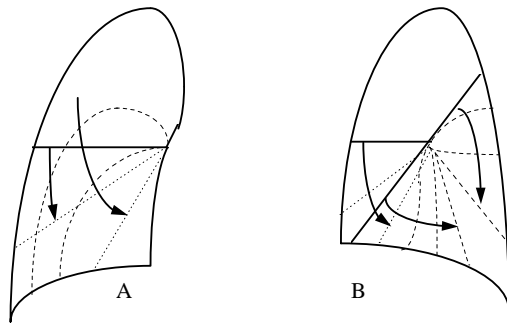


Fig.4. RLL atelectasis in progress

On CT scans, the RML is triangular or trapezoidal. Its posterior border, demarcated by the major fissure, is usually well defined because the major fissure crosses the scan plane almost perpendicularly. On the other hand, the interface between RML and RUL is often less distinct because of the dome-shaped contour of the minor fissure.

Lower Lobar Atelectasis

As the lower lobes become atelectatic, the lateral portion of the major fissure moves posteriorly toward the costophrenic angle and may be well delineated on the lateral radiograph. The medial portion of the ma-

ior fissure relates to the mediastinal wedge of pulmonary attachment. The wedge is frequently difficult to detect on the lateral radiograph except for a slight area of increased opacity extending from the posterior costophrenic angle toward the hilum. On PA radiographs, the lateral margin of the lobe may be ill- or well-defined, depending on whether or not the adjacent hyperexpanded lung has placed the fissural edge of the lower lobe tangential to the x-ray beam.

If marked atelectasis of the RLL has occurred, the triangular-shaped opacity may be difficult to detect through the mediastinum because of its small size. In LLL atelectasis, the involved lobe may appear as a left paraspinal mass instead of the more characteristic triangular shape with the apex at the hilum and the base at the left hemidiaphragm. The appearance of lower lobar atelectasis as a paraspinal mass is believed to result from incomplete attachment of the inferior pulmonary ligament to the hemidiaphragm [9] (Figs. 4 and 5) (Table 4).

On CT scans, the lower lobes lose volume in a posteromedial direction, pulling down the major fissure. The lateral portion of this fissure demonstrates a greater degree of mobility, because the medial portion is fixed to the mediastinum by the hilar structures and the inferior pulmonary ligament.

Table 3. Ancillary Radiographic Findings of Atelectasis of Right Middle Lobe

Fissural Reorientation	Inferomedial and superomedial displacement of minor and major fissures, respectively
Hilum	No change in size and position
Mediastinum	Lack of major mediastinal shift
Diaphragm	Elevated anteriorly
Bronchus	Air bronchogram of RML bronchi on PA and lateral views

Table 4. Ancillary Radiographic Findings of Lower Lobe Atelectasis

Fissural Reorientation	Inferoposterior displacement of both major and minor fissures
Hilum	Downward displacement, small size
Mediastinum	Obliteration of IVC and descending aorta shadow with RLL and LLL atelectasis, respectively
Diaphragm	Portions of each hemidiaphragm that abuts atelectatic lower lobe may be obscured
Bronchus	Vertical orientation of lower lobar bronchus in PA radiograph; posterior and downward displacement of ipsilateral upper lobar bronchus on lateral radiograph

Combined Lobar Atelectasis

Combined Atelectasis of the Right Middle and Lower Lobes

Because the bronchus intermedius is the common pathway to the right middle and lower lobes, a single localized lesion involving the bronchus intermedius gives rise to combined atelectasis of these lobes. The bronchus can be obstructed with a tumor, a foreign body, a mucous plug, or an inflammatory stricture [10].

On the PA radiograph, the atelectatic RLL obscures the right hemidiaphragm, whereas the atelectatic right middle lobe obscures the right cardiac border. Depression of both the major and minor fissures is present, the depression being most marked laterally. The fissures cross over each other; the major fissure assumes more vertical orientation than the minor fissure. However, both the right minor and major fissures are usually obscured within mediastinal shadow. Therefore, visualization of the right minor fissure should suggest the diagnosis of isolated atelectasis of the right lower lobe. Occasionally, the fissures may be seen as crossing double interface in close approximation on PA radiograph. On the lateral view, increased opacity is present throughout the lower part of the chest (Fig. 6) (Table 5).

On CT scans, the atelectatic RML and RLL occupy the lower hemithorax and abut the right cardiac border medially and the right hemidiaphragm inferiorly. The right major and minor fissures border the posterior and anterior margins of the atelectatic lobes, respectively. Complete combined RML and RLL atelectasis can be difficult to detect on PA and lateral radiographs. The diagnosis should be suspected in patients with a small right hilum and an apparently oligemic right lung which represents the hyperexpanded RUL.

Combined Atelectasis of the Right Upper and Middle Lobes

For combined atelectasis of the RUL and RML to occur, the bronchi of both lobes must be narrowed or

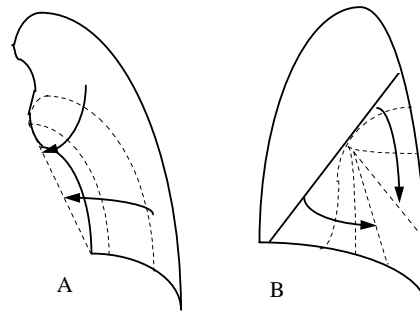


Fig.5. LLL atelectasis in progress

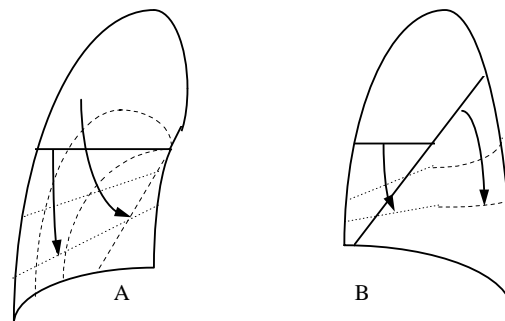


Fig.6. Combined RML and RLL atelectasis in progress

occluded by a single or two separate lesions while the bronchus intermedius remains patent, thus allowing the RLL to remain expanded. Combined atelectasis of the RUL and RML occurs most frequently in patients with bronchogenic carcinoma, in which the primary tumor can obstruct one bronchus and cause the other bronchus to be obstructed by direct extension through the lung parenchyma or peribronchial sheath or by lymphadenopathy [10].

On the PA radiograph, the atelectatic RUL and RML form an opacity that obscures the outline of the mediastinum and fades laterally. Combined atelectasis of the RUL and RML can lead to cephalad and lateral displacement and rotation of the hilar vessels.

Table 5. Ancillary Radiographic Findings of Combined Right Middle and Lower Lobe Atelectasis

Fissural Reorientation	Depression of both major and minor fissures, most marked laterally; right minor fissure is usually obscured within mediastinal shadow
Hilum	Small and depressed right hilum; decreased vascularity of hyperexpanded RUL compared with normal left lung
Mediastinum	Increased density in retrocardiac right lower lung zone due to atelectatic lobes
Diaphragm	Obliterated right hemidiaphragm due to atelectatic lobes, especially in lateral view
Bronchus	Medial displacement of bronchus intermedius

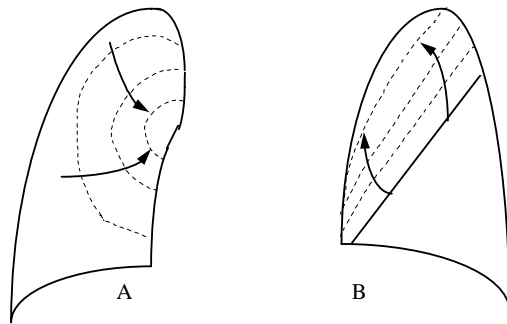


Fig.7. Combined RUL and RML atelectasis in progress

The silhouettes of the ascending aorta and the right atrium are usually obscured. On the lateral view, the major fissure can be seen displaced anteriorly. The relative proximity of the major fissure to the anterior chest wall is dependent on the degree of atelectasis of the RUL and RML. The radiographic findings of combined atelectasis of the RUL and RML are similar to those of LUL atelectasis [10] (Fig. 7) (Table 6).

On CT scan, the atelectatic RUL and RML cause a wedge-shaped area of soft-tissue attenuation abutting the chest wall anteriorly and the ascending aorta and right cardiac border medially. This wedge-shaped opacification extends inferiorly to the level of the right atrium. The major fissure is displaced anteriorly, and the hyperexpanded lower lobe fills most of the right hemithorax.

Combined Atelectasis of the Right Upper and Lower Lobes

Combined atelectasis of the RUL and RLL is rare. It may be due to mucous plugs occurring simultaneously in the bronchi of the RUL and RLL. The radiographic findings of combined atelectasis of RUL and RLL are similar to those of isolated atelectasis of either lobe. Upper lobe atelectasis leads to elevation of the minor fissure, whereas lower lobe atelectasis leads to downward and medial shift of the major fis-

sure. On CT scans, the minor fissure is higher than normal because of the atelectasis of the RUL and more posterior than normal because of the atelectasis of the RLL. The middle lobe is overinflated [10].

Peripheral Lobar Atelectasis

Franken and Klatter [11] described the radiographic findings of what they called “atypical (peripheral) right upper lobe atelectasis”, mimicking apical pleural effusion. In this type of atelectasis of the RUL, the atelectatic lobe continues to lie adjacent to the lateral chest wall. The dense portion of the atelectatic lobe is sharply margined medially. On CT in this form of atelectasis, the RML expands upward in front of the atelectatic RUL with the minor fissure adopting an almost coronal orientation. The superior segment of the RLL herniates upward posterior and medial to the atelectatic RUL with the major fissure being repositioned to a more parasagittal orientation superiorly, presenting itself as a radiographic interface on the PA projection [11-13]. The herniated superior segment of RLL forms the so-called Luftsichel (air crescent) medial to the atelectatic lobe. Recently two cases of peripheral atelectasis of left upper lobe, caused by bronchogenic carcinoma, have also been reported [13].

Migrating Lobar Atelectasis

A very heavy lobe, filled with fluid, chronic pneumonia, or a tumor, may migrate in the hemithorax with change in body position adopting a dependent position. Heavy lobes and pedunculated benign fibrous tumors of the pleura are the two likely causes of a large migrating chest density [10, 14]. Migrating atelectasis usually involves a single lobe (usually RUL), however it has also been described with combined RUL and RML atelectasis [15]. Migratory lobar atelectasis should be distinguished from lung torsion. Lobar migration is mainly a shifting process within the hemithorax, while lobar torsion is a rotatory or twisting process around its pedicle (bronchovascular bundle). Lobar migration has been regarded

Table 6. Ancillary Radiographic Findings of Combined Right Upper and Middle Lobe Atelectasis

Fissural Reorientation	Major fissure is be displaced anteriorly
Hilum	Cephalad and lateral displacement and rotation of hilar vessels
Mediastinum	Obscured outline medially and fades laterally
Diaphragm	Elevated with tenting
Bronchus	Obliterated bronchus intermedius due to tumor or mucus

to indicate a lobar torsion [16]. Some degree of torsion may be associated with lobar migration. However, on CT, twisted or obliterated bronchovascular bundles due to torsion are not usually seen in patients with lobar migration. Patients with lobar migration usually have no symptoms as in those with spontaneous lobar torsion, but differently from those with postoperative or posttraumatic torsion [15].

Rounded Atelectasis

Rounded atelectasis is a form of peripheral pulmonary volume loss. Rounded atelectasis is hypothesized to be due to contraction of a focus of visceral pleural fibrosis that results in buckling of the pleura and atelectasis of underlying lung parenchyma [17]. It usually results in volume loss of part of a lobe unrelated to the segmental anatomy. Rounded atelectasis usually presents as a mass that may simulate a pulmonary neoplasm on chest radiograph. The CT criteria for the diagnosis of rounded atelectasis include (1) a rounded or oval mass abutting a pleural surface, (2) vessels and bronchi curving into the mass, and (3) associated pleural thickening with or without calcification [18]. Although rounded atelectasis is usually confined to a small portion of lung, occasionally it may involve the entire lobe and simulate a large mass.

REFERENCES

1. Lee KS, Kim TS. Atelectasis. In: Taveras JM, Ferrucci JT, eds. Radiology, diagnosis-imaging-intervention. Vol. 1, Chap. 56. Philadelphia: Lippincott-Raven Publishers, 1998: 1-32
2. Mintzer RA, Sakowicz BA, Blonder JA. Lobar collapse. Usual and unusual forms. *Chest* 1988;94:615-620.
3. Lubert M, Krause GR. Further observations on lobar collapse. *Radiol Clin North Am* 1963;1:331-346.
4. Naidich DP, McCauley DI, Khouri NF, Leitman BS, Hulnick DH, Siegelman SS. Computed tomography of lobar collapse: 1. endobronchial obstruction. *J Comput Assist Tomogr* 1983;7:745-757.
5. Naidich DP, McCauley DI, Khouri NF, Leitman BS, Hulnick DH, Siegelman SS. Computed tomography of lobar collapse: 2. collapse in the absence of endobronchial obstruction. *J Comput Assist Tomogr* 1983;7:758-767.
6. Naidich DP, Ettinger N, Leitman BS, McCauley DI. CT of lobar collapse. *Semin Roentgenol* 1984;19:222-235.
7. Raasch BN, Heitzman ER, Carsty EW, Lane EJ, Verlow ME, Niter G. A computed tomographic study of bronchopulmonary collapse. *RadioGraphics* 1985;4:195-232.
8. Khoury MB, Godwin JD, Halvorsen RA, Putman CE. CT of lobar collapse. *Invest Radiol* 1985;20:708-716.
9. Glay J, Palayew MJ. Unusual pattern of left lower lobe atelectasis. *Radiology* 1981;141:331-333.
10. Lee KS, Logan PM, Primack SL, Müller NL. Combined lobar atelectasis of the right lung: imaging findings. *AJR* 1994;163:43-47.
11. Franken EA, Klatte EC. Atypical (peripheral) upper lobe collapse. *Ann Radiol* 1977;20:87-93.
12. Adler J, Cameron DC. CT correlation in peripheral right upper lobe atelectasis. *J Comput Assist Tomogr* 1988;12:510-511.
13. Donc C, Desmarais R. Peripheral upper lobe collapse in adults. *Radiology* 1989;170:657-659.
14. Heitzman ER. The lung: radiologic-pathologic correlation, 2nd ed. St. Louis: Mosby, 1984:457-501.
15. Kim TS, Lee KS, Hwang JH, Choo IW, Lim JH. Migrating lobar atelectasis of the right lung: radiologic findings in six patients. *Korean J Radiol* 2000;1:33-37
16. Felson B. Lung torsion: radiographic findings in nine cases. *Radiology* 1987;162:631-638.
17. Menzies R, Fraser R. Rounded atelectasis. Pathologic and pathogenetic features. *Am J Surg Pathol* 1987;11:674-681.

Recognition and Evaluation of Abnormal Cardiac Findings on Chest CT

Curtis E. Green, MD

Medical Center Hospital of Vermont

University of Vermont College of Medicine

Objectives

To describe and demonstrate the CT appearance of common cardiac abnormalities; the various pulmonary vascular patterns; complications of cardiac surgery; and primary and metastatic tumor to the heart.

Introduction

In the everyday practice of chest CT, one commonly encounters various cardiac findings that may not be recognized or fully understood. These may have been intentionally sought after or completely unsuspected. It is not the purpose of this lecture to try to describe the specialized techniques used to image the heart by CT, but rather to address those entities which one may encounter during the performance of routine chest CT.

Cardiac Calcification

Calcium may be seen in a number of locations in the heart. Most common of all is coronary calcium, which as has been extensively discussed, is indicative of atherosclerosis. Because CT is so sensitive to its presence, the specificity for significant obstruction is diminished compared to less sensitive techniques such as fluoroscopy unless one quantitates the amount of calcium.

Calcium in the mitral annulus is a common finding in elderly individuals and is generally of no clinical significance although it is occasionally associated with floppy mitral valve and mitral regurgitation. There are also a few case reports of massive mitral annular calcium interfering with mitral valve opening resulting in mitral stenosis. Mitral annular calcium is usually very dense and forms an incomplete ring around the mitral valve since there is no annulus where the mitral and aortic valves meet.

Calcium in the aortic valve should raise the suspicion of aortic valve stenosis. As with coronary calcium, the increased sensitivity of CT for calcium makes its presence less specific for aortic stenosis than when seen on chest radiographs. Unlike with the mitral valve, there is no true aortic valve annulus, so annular calcium is not a consideration. Thin, curvilinear calcium in the sinuses does not necessarily indi-

cate aortic stenosis, especially in elderly individuals.

Calcium in the left ventricular wall results from previous myocardial infarction and does not necessarily indicate either ventricular aneurysm or thrombus, although either could be present. The main differential diagnosis is pericardial calcium. If the calcium extends onto the right ventricle or left atrium, it is pericardial in location. Focal pericardial calcium over the left ventricle may be difficult to distinguish from myocardial calcium, but identification of the pericardium as a separate structure usually allows the distinction to be made. Ventricular calcium is usually curvilinear, but is occasionally amorphous.

Chamber Analysis

There are, unfortunately, no hard and fast guidelines for determining whether or not a specific cardiac chamber is normal in size or thickness. Part of the problem lies in the inherent limitations of CT, primarily that the transverse imaging plane does not usually correspond to the long or short axis of the heart and that the relatively long exposure times average cardiac motion. The result of the latter is that one can never be sure which phase of the cardiac cycle has been imaged on a given slice. Since both chamber size and ventricular wall thickness vary significantly during the cardiac cycle this poses a real problem. So, even if one assumes that the normal echocardiographic dimensions can be translated to CT studies, one cannot be certain that the measurements from the CT scan correlate with what one would find on a cardiac echo. At echo, normal short axis end diastolic LV diameter is 5.6 cm and normal anteroposterior LA diameter is 4.5 cm. One can say that a given chamber will likely be no smaller than measured, but it is difficult to be certain that the chamber is not in fact larger than apparent. Global cardiac size and CT ratio can certainly be evaluated more accurately with CT than with chest radiographs, but are subject to many of the same limitations. Both are affected by skeletal anomalies such as narrow AP thoracic diameter and pectus excavatum deformity, and by inspiratory effort. At least one should not be

confused by prominent pericardial fat imitating cardiomegaly as it frequently does on chest radiographs. Unfortunately the bottom line is that one mostly has to fall back on experience with what are normal chamber sizes and whether the venae cavae and azygous vein are distended.

All of these limitations should not keep one, however, from carefully looking for morphologic abnormalities since even routine CT may pick up ventricular aneurysms and thrombus as well as atrial clots and tumors. Ventricular aneurysms will usually be readily apparent when located anteriorly or laterally, but may be very difficult to recognize when inferior. Remember that anterior ventricular aneurysms are always true aneurysms, but inferior and posterior aneurysms may be either true aneurysms or pseudoaneurysms. Clots are more common in the LV than RV and usually “line” the cavity wall although they may protrude into the lumen. The latter have a higher likelihood of embolizing. Clots in the RV usually arise from the peripheral veins or are tumor thrombi. Intracavitary atrial tumor and clot may be difficult to distinguish. In general one will not see left atrial thrombus in the absence of obvious atrial enlargement. Right atrial thrombus may be continuous with clot from the inferior vena cava.

Tumor involvement of the heart can be either primary or secondary (metastatic), the latter being much more common. The most common primary benign tumors of the heart are the myxoma (intracavitary) and the rhabdomyoma (myocardial). Myxomas are most frequently found in the left atrium followed by the right atrium and right ventricle. They may be multiple. Most are relatively smooth and attached to the atrial septum. The frequently calcify, especially those in the right atrium. Rhabdomyomas cause either focal or diffuse left ventricular wall thickening. These are usually discovered in childhood and have an increased incidence in patients with tuberous sclerosis. Rhabdomyosarcoma is the most common primary cardiac malignancy.

Most cardiac tumor involvement is metastatic. Lung and breast are the most commonly encountered tumors owing to their high prevalence. Melanoma and lymphoma have the highest incidence of cardiac metastases, however. Most metastases involve the epicardium (parietal pericardium) and cause pericardial effusion as their primary finding. Deep myocardial invasion is occasionally seen, although much easier to recognize on MR scans than on CT scans. Mediastinal tumor involvement, especially from lung carcinoma, may compress the left atrium and pulmonary veins causing pulmonary edema. Lung carcinoma may also directly invade the pulmonary veins,

even extending into the left atrium. Lung and mediastinal tumors occasionally directly invade the heart.

Pulmonary Vascular Patterns

This discussion will be limited to the three most common pulmonary vascular patterns and not address decreased pulmonary blood flow or systemic to pulmonary collateral flow.

Pulmonary venous hypertension (PVH) is usually caused by elevation of left atrial pressure and is characterized hemodynamically by an elevated pulmonary capillary wedge pressure. On chest radiographs this is manifest initially as redistribution of pulmonary blood flow to the non-dependent lung zones (apices in the upright patient) followed by interstitial and then alveolar edema. On CT one sees similar findings although CT is considerably more sensitive than plain films. Because the patient is usually supine for chest CT, “redistribution” will result in prominence of the anterior (non-dependent) pulmonary vessels. As the patient develops interstitial edema one begins to see subpleural edema and ground glass opacity, the former appearing as smooth thickening of the fissures, peribronchovascular bundles and interlobular septa. Pleural effusions may also develop. Alveolar edema results in airspace consolidation. One usually sees a combination of findings with the worst involvement in dependent lung zones unless there is extensive underlying pulmonary disease, especially emphysema.

Pulmonary overcirculation (colloquially referred to as “shunt” vascularity) most frequently results from left-to-right cardiac shunts or chronic systemic volume overload states such as severe anemia. The most common shunt by far in the adult is the atrial septal defect (ASD). Partial anomalous pulmonary venous return (PAPVR), with or without associated ASD, is next most common. Patent ductus arteriosus, partial persistent atrioventricular canal and ventricular septal defect are rare in adults. With the exception of PAPVR, one is unlikely to make a specific diagnosis, but the CT findings often allow one to suggest the underlying physiology and recommend echocardiography for further evaluation. The key finding is that all of the pulmonary vessels are too big. This is easiest to recognize centrally, but analysis of the peripheral vessels is critical in distinguishing overcirculation from pulmonary arterial (precapillary) hypertension.

Pulmonary arterial hypertension (PAH) can result from backup of pressure from PVH (post capillary) or increased resistance in the pulmonary arterioles (precapillary). In the former case one will see the typical findings of PVH, and if the central vessels are enlarged the diagnosis should be mitral stenosis since most other causes of PVH do not result in chronic enough

elevation of pulmonary artery pressure to result in enlargement of the pulmonary trunk. In the case of pre-capillary pulmonary arterial hypertension, the key CT findings are enlargement of the pulmonary trunk and right and left main pulmonary arteries. This has been looked at in some detail and as it turns out one can diagnose PAH at CT with good specificity and moderate sensitivity. A recent study by Ng and colleagues¹ looked at the ratio of the diameter of the ascending aorta to that of the main pulmonary artery (pulmonary trunk) and main pulmonary artery diameter. They found that in patients under 50 years of age an Ao/PA ratio > 1 was the better predictor of PAH with a sensitivity of 70% and specificity of 92% for predicting a mean pulmonary artery pressure of >20 mm Hg. The positive and negative predictive values were 96% and 52% respectively. This was independent of body surface area. In older patients absolute PA diameter correlated better with PA pressure but was dependent on body surface area to some extent. Although other studies have found less solid correlation, it has been a consistent finding that there was some correlation between the size of the main PA and pulmonary arterial pressure. Because of the low sensitivity, however, one can never use a normal Ao/PA ratio or main PA diameter to exclude PAH.

Coronary Artery Abnormalities

In addition to identifying coronary calcium as a marker of coronary atherosclerosis, CT is occasionally useful for the identification of other coronary artery abnormalities. These include congenital anomalies of origin, native coronary aneurysms and coronary bypass graft aneurysms.

The most important congenital coronary anomaly is aberrant origin of either the left main coronary artery or the left anterior descending coronary artery from the right coronary artery. Thin sections through the aortic root on contrast enhanced scans will frequently demonstrate the left main or anterior descending arising from the right sinus of Valsalva and coursing to the anterior interventricular groove. Passage of the artery anterior to the pulmonary trunk is benign. Passage between the aorta and main PA, however, is associated with angina and sudden death. The most common coronary anomaly, aberrant origin of the left circumflex coronary from the right coronary, is almost always benign.

Aneurysms of the coronary arteries may be recognizable when either large and proximal, or calcified. These may be either atherosclerotic in origin or associated with Kawasaki's disease. Aneurysms may also form in saphenous vein coronary grafts. These may be saccular or fusiform and frequently calcify and fill

with thrombus. Knowledge of the normal course of vein grafts helps in recognition and allows one to suggest which graft is involved. Anterior descending grafts usually come off the front of the ascending aorta several centimeters above the aortic valve. Right coronary grafts typically arise from the right side of the aorta fairly near the sinus of Valsalva. Grafts to the left circumflex branches are usually above and slightly posterior to the right coronary grafts and course posteriorly.

Tetralogy of Fallot

The success of surgical repair of tetralogy of Fallot has resulted in a fairly large number of adults with a reasonably normal life span. Most of these will not have any remarkable CT findings although aneurysmal dilatation of the right ventricular outflow tract may develop, mostly in patients with pulmonary artery branch stenosis. Those patients with the severest form of tetralogy, pulmonary atresia with ventricular septal defect, are prone to a number of long-term complications and may come to CT for a number of reasons. The complete repair consists of closure of the VSD and reconstruction of the pulmonary outflow tract and main pulmonary artery with either a composite graft or aortic homograft in the pulmonary position. The composite grafts consist of a dacron tube with a prosthetic valve in its mid-portion. The valve will be considerably higher than the native pulmonary valve would be. The graft may calcify or be narrowed by clot. Stenoses may occur in the proximal portions of the right and left main pulmonary arteries. Aortic homografts have a tendency to early calcification, especially in children. Patients with this type of repair may develop right heart failure and tricuspid regurgitation resulting in enlargement of the right atrium, right ventricle and inferior vena cava. A universal finding is enlargement of the ascending aorta, but is expected and not abnormal unless a frank aneurysm develops. One may also see calcium in the ventricular septal patch. Preoperatively, systemic-to-pulmonary artery collaterals supplied the lungs. These are usually occluded surgically or by coils, but some may remain patent after successful operative repair. They can arise from the descending aorta or great vessels.

Conclusion

Although cardiac diseases seem to remain a mystery to the average radiologist, there are many common abnormalities that can be readily recognized on routine CT scans and require no great feats of mental gymnastics to understand. The first step, however, is to regard the heart as more than a spacer between the lungs.

Anterior Mediastinal Masses

Pierre D. Maldjian, MD

Objectives

The objectives of this presentation are to:

1. Review a radiological scheme for the boundaries of the anterior mediastinum.
2. Discuss the differential diagnosis for masses of the anterior mediastinum.
3. Review the clinical and imaging features of various anterior mediastinal lesions.

Introduction

Benjamin Felson devised a practical scheme for division of the mediastinal compartments based on the lateral chest radiograph. One draws a vertical line along the anterior border of the trachea and posterior border of the heart to the diaphragm and a second vertical line 1 cm posterior to the anterior border of the vertebral bodies. A mass is considered to be within the anterior mediastinum if its center is anterior to the first line, within the middle mediastinum if it lies between the two lines and within the posterior mediastinum if the center is located posterior to the second line. Notice that in this conception masses overlying the heart shadow are considered to be within the anterior mediastinum unlike that of Fraser and Pare.

In this presentation we will discuss the clinical and imaging features of anterior mediastinal masses. Much of the time the differential diagnosis for a tumor at a particular location can be deduced by simply asking the question "What lives there?" This is especially true of the anterior mediastinum. Therefore, we will discuss masses originating from the thyroid gland, thymus, lymphatic tissue and germ cell rests.

Thyroid Masses

Thyroid masses are located at the thoracic inlet and a typical characteristic is lateral or posterior deviation of the trachea. Thyroid goiters that extend downward into the mediastinum usually extend to the anterior mediastinum but can extend into the middle mediastinum and even posterior to the trachea. On CT a mass can be assumed to be of thyroid origin if it is connected to the cervical thyroid. With benign goiter portions of the mass will also be of high attenuation (due to the iodine content) and there is marked and prolonged enhancement as in the normal thyroid gland. Thyroid goiters may also appear inhomogeneous with cystic regions and contain punctate or curvilinear calcifications. Thyroid cancer can be indistinguishable from goiter but CT signs that suggest

malignancy include: marked irregularity of the gland contour, loss of mediastinal fascial planes, encasement of vessels and cervical or mediastinal adenopathy.

Thymic Lesions

Thymomas arise from thymic epithelial cells. Patients are usually greater than 40 years of age. Fifty percent of patients have a paraneoplastic syndrome most commonly myasthenia gravis. It is the presence of spread of the tumor beyond the thymic capsule rather than the histologic appearance that determines malignancy. Therefore, on CT we attempt to classify these tumors as invasive or noninvasive. On CT a thymoma presents as a focal mass in the region of the thymus and calcification is not uncommon. CT findings suggestive of invasion are: irregular tumor margins or invasion of mediastinal fat, invasion or encasement of vessels, irregular interfaces with lung tissue, extension of the mass across the midline and drop metastases to the pleura or pericardium. Thymomas rarely metastasize outside of the thorax.

There are two forms of thymic hyperplasia. True thymic hyperplasia is hyperplasia of the cortex and medulla and can be associated with Grave's disease, thyrotoxicosis, acromegaly and thymic rebound hyperplasia. On CT there is diffuse enlargement of the thymus but the overall shape is preserved. Thymic lymphoid hyperplasia occurs from proliferation of the medullary B-cell lymphoid follicles. This type of hyperplasia is strongly associated with myasthenia gravis and is the most common thymic abnormality associated with this disease. On CT the thymus may appear normal or diffusely enlarged.

Thymic cysts may be congenital or acquired. Acquired thymic cysts can result from inflammation of the thymus, cystic degeneration of the thymus or neoplastic involvement of the thymus. A thymic cystic mass can result from treatment of Hodgkin's lymphoma or represent a cystic component of a neoplasm. A nonneoplastic thymic cyst usually has the following features on CT: thin wall, homogeneous internal contents that measure fluid density, no associated mass and no enhancement.

Thymolipomas are slow growing hamartomatous lesions of the thymus that contain fat. These are usually incidental in young adult males. These masses are usually large but soft and pliable. They may drape around the heart and other mediastinal structures. On CXR a thymolipoma may appear as a large anterior

mediastinal mass that changes shape with position due to its pliable nature. The presence of regions of fatty attenuation on CT is characteristic.

Thymic carcinoid is a rare tumor that arises from cells of neuroendocrine origin. Fifty percent are functionally active most commonly producing ACTH resulting in Cushing's syndrome. This tumor is also associated with MEN syndromes I and II. These are aggressive tumors and 20% of patients have metastases at presentation. On CT this lesion may appear as a large anterior mediastinal mass that may be localized or invasive.

Thymic carcinoma is a rare neoplasm that arises from thymic epithelial cells. These lesions are more aggressive and more likely to metastasize than invasive thymomas. On CT this may appear as a large anterior mediastinal mass with poorly defined margins. Gross invasion of adjacent structures and mediastinal adenopathy is common.

Tumors of Lymphatic Origin

Eighty-five percent of patients with Hodgkin's lymphoma present with mediastinal adenopathy most commonly involving the prevascular and paratracheal nodes. The adenopathy is commonly bulky and massive on CT. The nodes are usually homogeneous but can be cystic and necrotic especially after treatment. Intrathoracic involvement is less common with non-Hodgkin's lymphoma but if there is intrathoracic disease the prevascular and paratracheal nodes are most commonly involved. Primary mediastinal large B-cell lymphoma is a subtype of NHL that may arise from thymic medullary B cells. This presents as a large lobulated anterior mass. Low attenuation regions from necrosis is common on CT.

A lymphangioma is a congenital malformation of the lymphatic system composed of lymph channels or cystic lymph spaces. Lymphangiomas most commonly occur in the neck and can extend to the mediastinum. These usually present in infancy. Lymphangiomas confined to the mediastinum are rare and usually present in older children and adults. On CT this is seen as a unilocular or multilocular mass of fluid attenuation that may mold to or envelop adjacent mediastinal structures. Septations may also be present.

Mediastinal Germ Cell Tumors

The anterior mediastinum is the most common extragonadal site for germ cell tumors. These arise from germ cell rests in the mediastinum. With benign germ cell tumors the incidence in males and females is about equal but malignant tumors occur almost exclusively in males. These lesions can be classified as teratomas, seminomas or nonseminomatous malignant germ cell tumors.

Mediastinal teratoma is the most common mediastinal germ cell tumor. Most cases represent benign mature teratomas. The production of digestive enzymes from pancreatic tissue or intestinal mucosa within the tumor can cause rupture into the lung, airways, pericardium or pleura. Trichoptysis (coughing up hair) is a rare but characteristic symptom of ruptured mediastinal teratoma. On CT, this lesion commonly appears as a multilocular cystic mass that may contain fluid, soft tissue, calcium and fat. A fat-fluid level is a specific finding but is only seen in 11% of cases.

Mediastinal seminoma is a tumor of young adult males (average age = 29). On CT this tumor usually appears as a large homogeneous soft tissue mass. The margins are usually well defined but there can be invasion of adjacent structures. Cystic elements may be present. Nonseminomatous malignant germ cell tumor of the mediastinum is also a tumor of young males. On CT this may appear as a large heterogeneous mass due to necrosis and hemorrhage. There is often infiltration of surrounding tissue with obliteration of tissue planes and invasion of adjacent structures. Twenty percent of these patients have Klinefelter's syndrome (47, XXY).

Ectopic Parathyroid Adenoma

In patients with primary hyperparathyroidism surgical neck exploration with resection of parathyroid tissue is curative in 90-95%. Persistence of hyperparathyroidism after surgery suggests ectopic parathyroid tissue. Fifty percent of these patients will have a mediastinal ectopic parathyroid gland. In 2/3 of cases the ectopic mediastinal parathyroid gland is located in the superior mediastinum near the tracheoesophageal groove but in 1/3 it is found in the anterior mediastinum within the thymus. On CT an ectopic anterior mediastinal parathyroid adenoma appears as a small homogeneous enhancing mass. On MRI this lesion is characteristically markedly hyperintense on T2 weighted images.

Conclusion

We have discussed some of the characteristic clinical and imaging features of various anterior mediastinal masses. However, in our approach to mediastinal lesions we must remember to consider common pathological entities. The possibilities of a vascular lesion such as an aneurysm or lung cancer invading the mediastinum should always be entertained especially when a mediastinal mass is first encountered on a chest radiograph before any cross sectional imaging has been performed. After cross sectional imaging has been done, in addition to the appearance of the lesion, clinical information is also vital for formulating a pertinent differential diagnosis.

BIBLIOGRAPHY

1. Strollo DC, Rosado-de-Christenson ML. State of the Art: Tumors of the Thymus. *Journal of Thoracic Imaging* 1999; 14: 152-171.
2. Strollo DC, Rosado-de-Christenson, Jett JR. Primary Mediastinal Tumors Part I: Tumors of the Anterior Mediastinum. *Chest* 1997; 112: 511-522.
3. Brown LR, Aughenbaugh GL. Masses of the Anterior Mediastinum: CT and MR imaging. *AJR* 1991; 157: 1171-1180.
4. Tecce PM, Fishman EK, Kuhlman JE. CT Evaluation of the Anterior Mediastinum: Spectrum of Disease. *Radiographics* 1994; 14: 973-990.
5. Moeller KH, Rosado-de-Christensen ML, Templeton PA. Mediastinal Mature Teratoma: Imaging Features. *AJR* 1997; 169: 985-990.
6. Naidich DP, Webb WR, Muller NL et al. Mediastinum. In: *Computed Tomography and Magnetic resonance of the Thorax* 3rd ed. Philadelphia: Lippincott-Raven 1999: 37-159.

Pulmonary Aspergillosis: An Interconnected Spectrum

Irwin M. Freundlich, MD

Aspergillus is a ubiquitous fungus, which attacks the immunocompetent, hypersensitive individual, the chronically ill as well as the immunosuppressed patient. Although the same fungus is responsible, the manifestations of disease are quite disparate. The immune system of the host plays the critical role. We are indebted to Warren Geffer, Wallace Miller and others of the University of Pennsylvania group for shedding much light on this subject (ref.1).

Pulmonary aspergillosis afflicts three very different groups of patients; those with (1) allergic bronchopulmonary aspergillosis (ABPA), (2) a mycetoma or (3) invasive aspergillus infection. However, there is an overlap or interconnection between ABPA and the mycetoma in that a dilated bronchus found in the former may act as the preexisting space in which a mycetoma develops. This occurs in about 7% of ABPA patients (ref.2). Semi-invasive aspergillosis occurs in chronically ill or debilitated patients who have a mycetoma and whose immune systems are not entirely normal. These patients are much less ill but are in some respects similar to immunosuppressed patients with invasive aspergillosis.

Allergic Bronchopulmonary Aspergillosis

ABPA occurs in 1 to 2% of asthmatic patients and 96% of ABPA patients have asthmatic symptoms. It is uncertain but possible that in those patients the fungus itself is the initiating cause of the asthma. Although *Aspergillus fumigatus* is most common, other species of *Aspergillus* and rarely other fungi may be responsible (ref.2). Laboratory data necessary for the diagnosis of ABPA from reference 2 are as follows:

A. Primary

1. Immediate skin test positive*
2. Precipitating antibodies pos. for *A. fumigatus*
3. Elevated IgE and serum spec. IgE and IgG
4. Eosinophilia of less than 40%

B. Secondary

1. *Aspergillus* found in sputum
2. Expectoration of plugs
3. Delayed skin test pos. (Arthus)

*critical for diagnosis

The pathology consists of a unique and specific dilatation of middle order bronchi and bronchocentric granulomatosis. The mycelia of *Aspergillus* should be seen immediately following bronchoscopy because the fungus often appears as a contaminant in laboratory cultures.

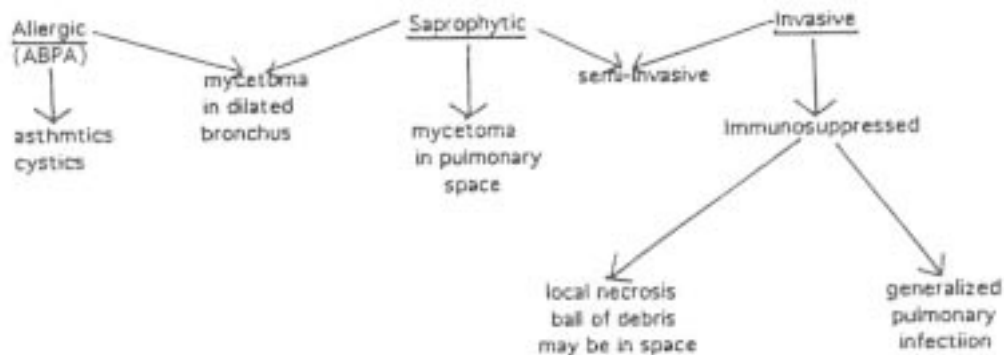
ABPA is often manifested by an acute flu-like illness with fever and headache. In later chronic stages dyspnea and cyanosis may be seen. Five stages have been described (ref.2).

1. Acute illness
2. Radiographic clearing, IgE declines
3. Acute illness reappears
4. Steroid dependency
5. Irreversible lung damage

Early in the acute phase the radiographic appearance of a transitory pneumonitis is nonspecific but later the radiographs are often typical and diagnostic.

Radiographic Criteria

1. Transient pneumonitis
2. DILATATION OF MIDDLE ORDER BRONCHI
 - a. empty air filled
 - b. containing mucus plugs
3. Thick bronchial walls
4. A mycetoma in a dilated bronchus



Mycetoma

A mycetoma consists of a ball of mucus containing a fungus, in this case the mycelia of *Aspergillus*. The aspergilloma is the most common fungus ball and the species *fumigatus* is much more frequently found in this country than any other. A mycetoma may be found in ANY abnormal pulmonary space. Except for those found in the dilated bronchi of ABPA, the space is the result of a previous or pre-existing pulmonary disease. Mycetomata have been found in cavities secondary to healed abscesses or tuberculosis, in the cystic spaces of stage 3b sarcoidosis, in pneumatoceles from a gunshot wound, in primary and secondary neoplastic cavities, as well as emphysematous bullae.

Hemoptysis is common and the most life threatening complication of a mycetoma. In one series 70% of 26 patients experienced hemoptysis and two exsanguinated (ref.3). Surgical resection is recommended for those who can tolerate the procedure; otherwise aggressive medical management is necessary.

Although the mycetoma may be seen on routine radiographs, any patient with chronic cystic disease and hemoptysis should have a CT examination not only for confirmation but, particularly prior to surgery, to be sure only one mycetoma is present. Those with a solitary cavity may not need CT if the mycetoma can be seen in the cavity or if surgery is planned anyway. (Whether the fungus ball moves within a cavity on decubitus radiographs has no importance).

Semi-invasive Aspergillosis

This unusual group of patients falls between those with a quiescent mycetoma and the invasive infection seen in immunocompromised patients (ref.1). A chronic debilitating disease such as diabetes, alcoholism, COPD, neoplasm, etc. lowers the immune response. A mycetoma may be present but in these cases the wall of the cavity and surrounding lung are slowly invaded by the organism. A local area of consolidation results adjacent to the cavity. A recent report of nine COPD patients with semi-invasive aspergillosis found consolidation in six but multiple nodules in an additional three (ref.4).

Invasive Aspergillosis

Invasive aspergillosis is a life threatening disease in immunocompromised patients. Leukemics are the most susceptible but any patient with bone marrow

suppression is at risk. The following data were derived from 61 patients at the M.D. Anderson Center:

Primary Neoplasm	Histology
leukemia-----55.7%	AML-----21.3%
lymphoma-----16.4%	ALL-----13.1%
multiple myeloma - 3.3%	myelodys.—13.1%
reticuloendothel.---14.8%	CML----- 9.8%
other neoplasms--- 9.8%	CLL----- 8.2%
	other neo.—29.6%

Locally necrotic invasive aspergillosis presents the most recognizable radiographic images. Usually this phase of the disease is seen after partial bone marrow recovery. About three thousand white cells are needed to successfully wall-off the infection. The following radiographic findings may be seen:

1. Air and/or fluid filled cavity(s)
2. A ball of debris may be seen in the cavity (not a mycetoma)*
3. Ulceration of the bronchial mucosa

*although mycelia may be found in the ball of necrotic pulmonary tissue within the cavity, the term mycetoma has been assigned to a different kind of patient with a much more manageable and less life threatening disease.

Diffuse invasive aspergillosis is seen in those immunocompromised patients who are unable to mount a sufficient defense and the prognosis is poor. The radiographic picture is usually not as recognizable. Multiple nodules or patches of non-descript infection lead to diffuse air-space filling. The radiographs or scans may present a picture indistinguishable from other infections.

Either locally invasive or diffuse aspergillosis may invade the pericardium resulting in pericarditis and either may induce significant hemorrhage that may make emergency surgery necessary.

BIBLIOGRAPHY

1. Geffer, W. The Spectrum of Pulmonary Aspergillosis. *J Thor Imag* 1992; 7(4):56-74.
2. Zhaoming, R.F., Lockey, L. A Review of Bronchopulmonary Aspergillosis. *J Invest Allergol Clin Immunol* 1996; 6:144-151.
3. Freundlich, I.M., Israel, H.L. Pulmonary Aspergillosis. *Clin Rad* 1973; 24:248-253.
4. Fanquet, T., Muller, N.L. et al. Semiinvasive Aspergillosis in Chronic Obstructive Pulmonary Disease; Radiologic and Pathologic Findings in Nine Patients. *AJR* 2000;174:51-56.

Notes

A large, empty rectangular area with a dark border, intended for taking notes. The border is composed of a vertical line on the left and a horizontal line at the bottom, meeting at a rounded corner. The interior of the rectangle is completely blank white space.